White matter microstructural changes in short-term learning of a continuous visuomotor sequence

Tremblay, S.A.; Jäger, A.-T.; Huck, J.; Giacosa, C.; Beram, S.; Schneider, U.; Grahl, S.; Villringer, A.; Tardif, C.L.; Bazin, P.-L.; Steele, C.J.; Gauthier, C.J.

DOI
10.1007/s00429-021-02267-y

Publication date
2021

Document Version
Final published version

Published in
Brain Structure and Function

Brain Structure and Function (2021) 226:1677–1698
https://doi.org/10.1007/s00429-021-02267-y

ORIGINAL ARTICLE

White matter microstructural changes in short-term learning of a continuous visuomotor sequence

Stéfanie A. Tremblay[1,2] · Anna-Thekla Jäger[3,11] · Julia Huck[1] · Chiara Giacosa[1] · Stephanie Beram[1] · Uta Schneider[3] · Sophia Grahl[3] · Arno Villringer[3,4,5,6] · Christine L. Tardif[7,8] · Pierre-Louis Bazin[3,9] · Christopher J. Steele[3,10] · Claudine J. Gauthier[1,2]

Received: 4 October 2020 / Accepted: 26 March 2021 / Published online: 22 April 2021

Abstract

Efficient neural transmission is crucial for optimal brain function, yet the plastic potential of white matter (WM) has long been overlooked. Growing evidence now shows that modifications to axons and myelin occur not only as a result of long-term learning, but also after short training periods. Motor sequence learning (MSL), a common paradigm used to study neuroplasticity, occurs in overlapping learning stages and different neural circuits are involved in each stage. However, most studies investigating short-term WM plasticity have used a pre-post design, in which the temporal dynamics of changes across learning stages cannot be assessed. In this study, we used multiple magnetic resonance imaging (MRI) scans at 7 T to investigate changes in WM in a group learning a complex visuomotor sequence (LRN) and in a control group (SMP) performing a simple sequence, for five consecutive days. Consistent with behavioral results, where most improvements occurred between the two first days, structural changes in WM were observed only in the early phase of learning (d1–d2), and in overall learning (d1–d5). In LRNs, WM microstructure was altered in the tracts underlying the primary motor and sensorimotor cortices. Moreover, our structural findings in WM were related to changes in functional connectivity, assessed with resting-state functional MRI data in the same cohort, through analyses in regions of interest (ROIs). Significant changes in WM microstructure were found in a ROI underlying the right supplementary motor area. Together, our findings provide evidence for highly dynamic WM plasticity in the sensorimotor network during short-term MSL.

Keywords White matter · Plasticity · DWI · DTI · Fractional anisotropy (FA) · Motor sequence learning

Introduction

The idea that structure determines function, and that function can modulate structure, is a well-known concept governing biology (Kohn et al. 2018). Just like any other organ in the body, the structure of the brain changes in response

Christopher J. Steele and Claudine J. Gauthier contributed equally to this work.

✉ Claudine J. Gauthier
Claudine.Gauthier@concordia.ca

1 Department of Physics/PERFORM Center, Concordia University, Montreal, QC, Canada

2 Montreal Heart Institute, Montreal, QC, Canada

3 Department of Neurology, Max Planck Institute for Human Cognitive and Brain Sciences, Leipzig, Germany

4 Clinic for Cognitive Neurology, Leipzig, Germany

5 Leipzig University Medical Centre, IFB Adiposity Diseases, Leipzig, Germany

6 Collaborative Research Centre 1052-A5, University of Leipzig, Leipzig, Germany

7 Department of Biomedical Engineering, McGill University, Montreal, QC, Canada

8 Montreal Neurological Institute, Montreal, QC, Canada

9 Faculty of Social and Behavioral Sciences, University of Amsterdam, Amsterdam, Netherlands

10 Department of Psychology, Concordia University, Montreal, QC, Canada

11 Charite Universitätsmedizin, Charite, Berlin, Germany

to changing demands in order to support new functions, in a process termed neuroplasticity (Zatorre et al. 2012). Synaptic changes have been the main focus of early plasticity studies (Rioult-Pedotti et al. 2000; Xu et al. 2009), yet recent research now indicates that plastic changes can also involve alterations to neurons, glial cells, and cerebral vessels (Sampaio-Baptista and Johansen-Berg 2017; Tardif et al. 2016; Zatorre et al. 2012).

The plastic potential of white matter (WM), and the behavioral relevance of changes in the fiber tracts connecting neurons, has long been overlooked. However, growing evidence now shows modifications to astrocytes, microglia, and myelin-producing oligodendrocytes occur as a result of experience-dependent learning (Chorghay et al. 2018; Tardif et al. 2016). There is a large amount of evidence regarding activity-dependent myelination (Caeyenberghs et al. 2016; Lakhani et al. 2016; Sampaio-Baptista et al. 2020; Sampaio-Baptista and Johansen-Berg 2017 for review) and some studies have also shown that axonal diameter can change in adult brains (Chéreau et al. 2017; Lazari et al. 2018; Lee et al. 2012). Changes to axons and myelin would lead to changes in conduction speed and thus more efficient information processing through optimized timing of neural transmission (Chorghay et al. 2018; Fields 2015; Sampaio-Baptista and Johansen-Berg 2017). Given the crucial role of efficient neural transmission for optimal brain function (Fields 2015; Waxman 1975), a deeper understanding of the ways in which WM can be altered by experience is of critical importance.

Motor sequence learning (MSL) tasks are a common paradigm used to study neuroplasticity (Doyon et al. 2009; Hikosaka et al. 2002; Nissen and Bullemer 1987; Penhune and Steele 2012) MSL occurs in overlapping stages that have been described by various models. As such, motor learning can be divided into an initial fast stage, where a large amount of improvement occurs in a short period of time, followed by a consolidation stage, which solidifies the gains in performance between training sessions, making them resistant to interference. In a final late/slow stage, the learned sequence is fine-tuned to optimize motor parameters such as force, timing and spatial accuracy (Dayan and Cohen 2011; Doyon et al. 2002; Doyon and Benali 2005; Karni and Sagi 1993; Korman et al. 2003; Luft and Buitrago 2005). In each case, there is significant evidence from neuroimaging studies that different neural circuits are involved in each stage of learning (see Dayan and Cohen 2011; Halsband and Lange 2006 for reviews).

Studying neuroplasticity with magnetic resonance imaging (MRI) allows for the longitudinal investigation of functional and structural reorganization at the network (how are different brain regions connected to each other, i.e., whole-brain level) and microstructural levels (what properties do the fiber bundles that make up these connections have, i.e., voxel level), as whole-brain images can be obtained repeatedly (Tardif et al. 2016). Recent advances in MRI techniques and models, especially in the areas of connectivity and network theory, have created the opportunity for a better understanding of how brain architecture and network efficiency impact information processing and how these are modified through experience (Albert et al. 2009; Guye et al. 2010; Lewis et al. 2009). Changes in connectivity can be defined structurally, with diffusion-weighted imaging (DWI), a technique that probes WM microstructural organization through imaging the bulk motion of water molecules (Abdul-Kareem et al. 2011; Klein et al. 2019; Le Bihan et al. 2001), and functionally, through the measurement of spontaneous activity at rest and the temporal correlation of the blood-oxygen-level-dependent (BOLD) signal between brain regions (resting-state functional MRI) (Albert et al. 2009; Lewis et al. 2009).

In parallel, advances in hardware, such as the increasing use of ultra-high field MRI, and improved modeling approaches allow for the characterization and quantification of several properties of brain structures at finer spatial scales (Dumoulin et al. 2018; Frangou et al. 2020; Heidemann et al. 2012). These advances could allow us to bridge the gap between the knowledge gained from animal and human studies, and better define the mechanisms and time course at play when the brain is reshaped through experience (Sampaio-Baptista and Johansen-Berg 2017; Tardif et al. 2016).

Although the greatest gains in performance occur during the initial stage of learning (Dayan and Cohen 2011; Halsband and Lange 2006; Savion-Lemieux and Penhune 2005), early investigations of WM plasticity mainly focused on the effects of long-term training with cross-sectional studies in musicians and dancers with several years of training (Abdul-Kareem et al. 2011; Bengtsson et al. 2005; Giacosa et al. 2016, 2019; Hänggi et al. 2010). The cross-sectional nature of many of these studies does not allow characterization of the temporal dynamics of learning nor distinguishing training-induced changes from pre-existing differences in WM (e.g., Abdul-Kareem et al. 2011; Bengtsson et al. 2005; Giacosa et al. 2016, 2019; Hänggi et al. 2010; Steele et al. 2012). More recently, longitudinal studies using DWI have shown that WM changes can occur at shorter timescales. For instance, changes to WM microstructure underlying the intraparietal sulcus were observed after 6 weeks of juggling training (Scholz et al. 2009) and another study reported such changes in the fornix as quickly as after a few hours of spatial learning in a car racing game (Hofstetter et al. 2013). However, most studies investigating short-term WM plasticity have used a pre-post design, or a single measurement at the end of learning, in which the temporal dynamics of changes across learning stages cannot be assessed (Hofstetter et al. 2013; Scholz et al. 2009; Steele et al. 2012). Moreover, the control group in some of these studies does not allow to distinguish changes due to sequence-specific learning from

those due to motor execution (e.g., Scholz et al. 2009). In this study, we used multiple MRI scans at 7 T to investigate changes in WM across learning stages in a group learning a complex visuomotor sequence, and in a control group performing a simple sequence. The DTI model used to derive diffusivity metrics from DWI data yields measures that are highly sensitive to changes in WM microstructure, although physiologically non-specific (Riffert et al. 2014). Moreover, we investigated WM plasticity in regions of interest (ROIs) near areas of change in functional connectivity, assessed with resting-state fMRI (rs-fMRI) data in the same cohort (Jaeger et al. 2021).

Methods

Participants

Forty neurologically normal individuals of 21–30 years of age (M ± SD: 24.5 ± 2.44; 21 females) and without motor or correctible visual impairments were recruited from the participant database of the Max Planck Institute for Human Cognitive and Brain Sciences in Leipzig, Germany. All participants were task naïve prior to this study and right-handed according to the Edinburgh Handedness Inventory (M ± SD: 83.7 ± 16.9), except for one who was ambidextrous (EHI = 40). The majority of participants had no exceptional musical experience (M ± SD: 8.55 ± 8.83 years), but one participant self-identified as a professional musician and two as having advanced musical experience. Participants had an average sport experience of 5.83 ± 7.15 years and two participants self-identified as professional athletes. After ensuring the participants had no neurological conditions and no contraindication to MRI, they gave written informed consent according to the declaration of Helsinki. Participants were randomized into two groups: the experimental group ($N = 20$), who learned a complex visuo-motor sequence, and the control group ($N = 20$), who learned a simple repetitive visuo-motor sequence. One participant from the experimental group was excluded from this study due to a large signal drop in DWI data. Table 1 shows the demographic data for each group. After completion of the study, participants were financially compensated for their time. The study was approved by the ethics review board of the Medical Faculty of the University of Leipzig and all participants provided written informed consent according to the Declaration of Helsinki.

Motor sequence learning task

The sequential pinch force task (SPFT) is a complex visuomotor sequence learning task requiring fine force control (Camus et al. 2009; Krakauer et al. 2019), and was previously shown to result in short-term plastic changes in grey matter (Gryga et al. 2012). During the SPFT, participants hold a pressure sensor between the thumb and index finger of their right hand (Fig. 1a) and are required to exert force on the sensor to match the height of a moving reference bar (REF; blue on Fig. 1b) displayed on a computer screen. Another moving bar (FOR; yellow), representing the amount of pressure they are exerting on the device, is also displayed on the screen to provide visual feedback. The device samples force continuously throughout the task at a rate of 80 Hz. The change in height of the REF bar follows one of two specific sequences, as illustrated in Fig. 1c. In the learning condition (LRN), the bar moves following a complex

Table 1 Demographic data in each group

	Group		Sex		Age	EHI (handedness)	Music years (formal)	Sport years (formal)
N	LRN	19	Male	9				
			Female	10				
	SMP	20	Male	10				
			Female	10				
	Missing	1						
Mean	LRN				25.1	84.8	7.87	4.95
	SMP				23.9	83.0	9.32	6.95
SD	LRN				2.47	18.0	8.29	6.97
	SMP				2.38	16.5	9.66	7.42
Min	LRN				22	40.0	0	0
	SMP				21	40.0	0	0
Max	LRN				30	100	28.0	25
	SMP				30	100	29.5	25

LRN experimental group, *SMP* control group, *SD* standard deviation, *EHI* Edinburgh Handedness Inventory

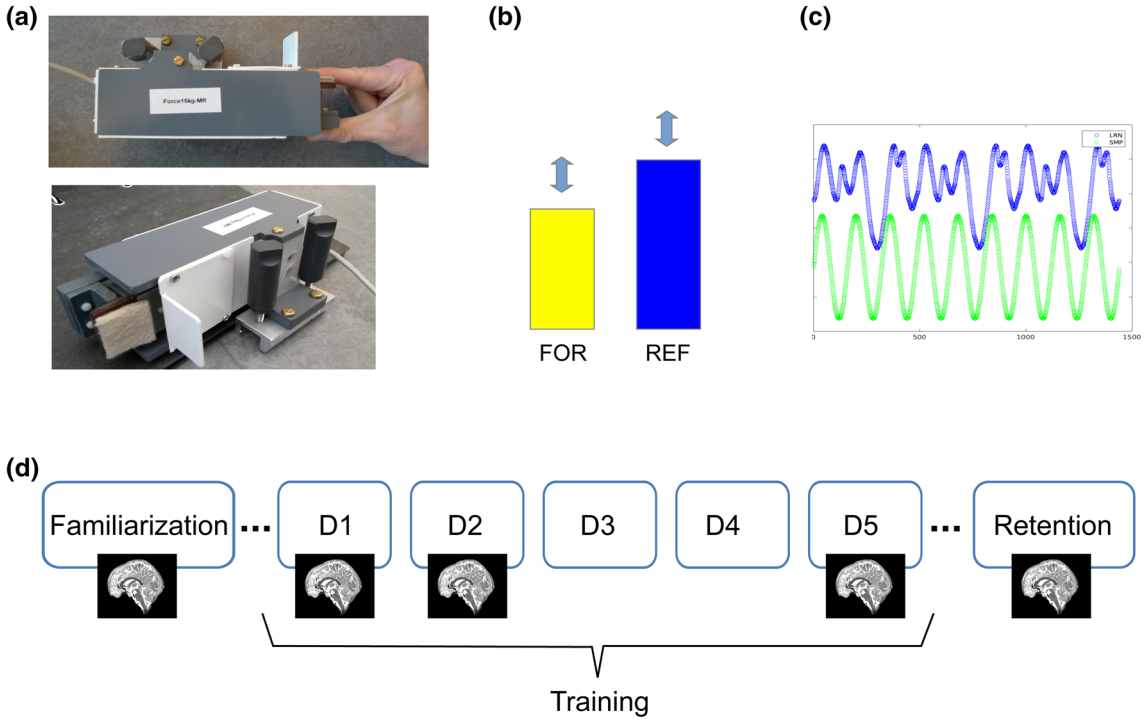

Fig. 1 Sequential pinch force task (SPFT) and experimental design. **a** SPFT device. Participants hold the pressure sensor between the thumb and index finger. **b** They exert force on the sensor to match the height of the reference bar (REF; blue). The FOR bar (yellow) represents the amount of force they are exerting on the device. **c** Visual representation of the complex (LRN; blue) and of the simple (SMP; green) sequences. **d** Schema of the experimental design. The familiarization session (d0) takes place 2 days before the first day of training (d1) and the retention scan (d17) 12 days after the last training day (d5). All training sessions (d1–d5) take place on consecutive days, Monday–Friday. Participants were in the scanner on d0, d1, d2, d5, and d17

sequence that is difficult to predict (blue on Fig. 1c) (Gryga et al. 2012). In the control condition, the bar moves following a simple sinusoidal sequence (SMP) that is learned almost immediately (green). The SMP sequence was designed to match the LRN sequence in terms of the total magnitude of force, duration, and frequency at the maximum level of force. This control condition can be used to distinguish between potential structural alterations related to motor execution (i.e., participants pinch a device in both conditions) from alterations that are specific to learning a sequence. Lastly, in the rest condition (RST), participants were asked to fixate their gaze on the static REF and FOR bars (both at 50% of their maximal height).

Experimental design

The experimental design is illustrated in Fig. 1d. Participants performed the SPFT on five consecutive days (Monday–Friday). A familiarization session (d0) on the previous Thursday or Friday, two days prior to the first day of training, allowed to test the participant's maximum pinch force and calibrate the level of force required in subsequent training sessions to avoid fatigue. The minimum bar level corresponded to a force of 5% of the participant's maximum force, while the maximum bar level corresponded to 30% of the participant's maximal force. During this session, participants also became familiar with the device and the task as they performed nine trials of the SMP sequence. Each training day (d1–d5), participants of the experimental group completed three pseudo-randomly presented blocks each consisting of three trials of SMP, RST, and LRN, resulting in a total of nine trials per condition every day. Participants in the control group also performed three blocks of training, but LRN trials were replaced by SMP trials. Throughout this manuscript, the experimental group will be referred to as the LRN group and the controls as the SMP group. Each trial lasted 18 s and the entire training session lasted 20 min as in Gryga et al. (2012). Participants were given feedback on their performance (i.e., average accuracy in matching the height of the REF bar) after the SMP and the LRN trials. A retention session (d17) was conducted approximately 12 days after the last day of training and consisted in the same procedure as the previous training sessions (d1–d5). The task was performed inside the MRI scanner on d0, d1, d2, d5, and d17 and outside the scanner on d3 and d4 (see Fig. 1d). Both MRI sequences of interest for this study (i.e., DWI and rs-fMRI) were acquired prior to SPFT training. All sessions for all participants took place in the morning

to avoid the potential influence of circadian rhythms on our results as the time of the day has been shown to impact the relative volumes of the intra-axonal and extra-axonal spaces in WM (Voldsbekk et al. 2020).

MRI acquisitions

MRI data were acquired on a Siemens 7 T scanner (MAGNETOM, Siemens Healthcare, Erlangen, Germany) with a 32-channel Nova head coil at the Max Planck Institute in Leipzig, Germany. DWI data, acquired from an Echo Planar Imaging (EPI) sequence (TR = 10,100 ms, TE = 62.8 ms, FOV = 192 × 192 mm^2, slice acceleration factor 2, slice thickness = 1.2 mm, 102 slices, GRAPPA factor 2, partial Fourier 6/8, b = 1000 s/mm^2, 20 directions, PE = AP, bandwidth = 1562 Hz/Px, voxel size = 1.2 × 1.2 × 1.2 mm), was used to assess WM microstructure. Rs-fMRI data were acquired with a blood-oxygen-level-dependent (BOLD) sequence (TR = 1130 ms, TE = 22 ms, flip angle = 40°, FOV = 192 × 192 mm^2, slice thickness = 1 mm, 102 slices, GRAPPA factor 2, partial Fourier 6/8, bandwidth = 1562 Hz/Px, voxel dimensions = 1.2 × 1.2 × 1.2 mm). Participants had their eyes open and were fixating their gaze on a cross during this 10-min acquisition. Rs-fMRI and DWI data were acquired prior to SPFT training. Uniform intensity T1-weighted images (UNI) were also acquired with an MP2RAGE sequence (TR = 5000 ms, TE = 2.45 ms, flip angle 1 = 5°, flip angle 2 = 3°, FOV = 224 × 224 × 240 mm^3, slice thickness = 0.7 mm, 240 slices, bandwidth = 250 Hz/Px, voxel size = 0.7 × 0.7 × 0.7 mm) (Marques et al. 2010). Fieldmaps were also acquired (TR = 18 ms, TE1 = 4.08 ms, TE2 = 9.18 ms, flip angle = 10°, FOV = 256 × 256mm^2, slice thickness = 2 mm, 80 slices, bandwidth 1 = 300 Hz/Px, bandwidth 2 = 300 Hz/Px, voxel dimensions = 2 × 2 × 2 mm) to correct distortions in BOLD images due to field inhomogeneities. As indicated above, one subject from the LRN group was excluded because of a large DWI signal drop in the temporal lobe.

Image preprocessing

DWI data were preprocessed using the MRtrix (3.0) software which performs denoising of the data, corrects for motion and Eddy currents (Eddy tool in FSL 6.0.1), and for susceptibility-induced distortions (topup tool in FSL) using b0 volumes of opposite phase-encoding polarities

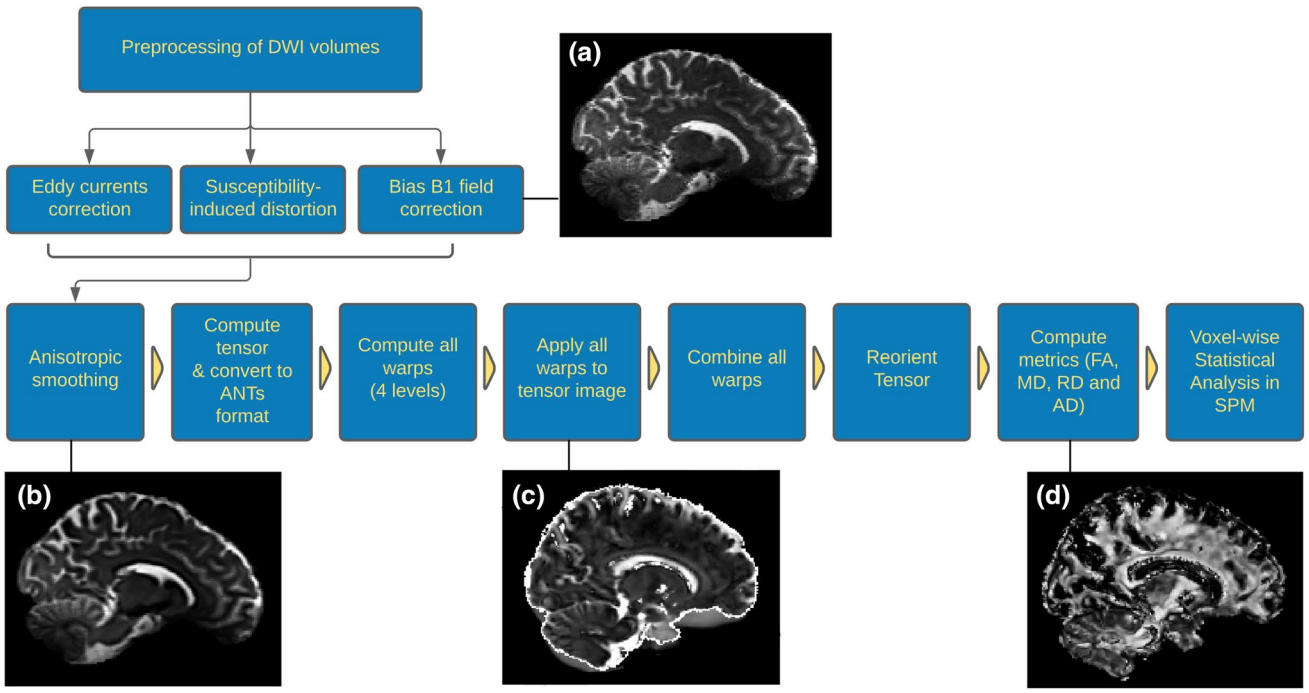

Fig. 2 DWI data processing workflow. Preprocessing included correction for motion, Eddy currents, susceptibility-induced distortions, and bias B1 field correction (N4). The preprocessed DWI image (b = 0 volume) of one participant is shown in **a**. Preprocessed DWI volumes were then smoothed anisotropically (**b**), fitted to a tensor model and converted to a symmetric matrix in the lower-triangular ordering (dxx, dxy, dyy, dxz, dyz, dzz) for ANTs. Four levels of warps were computed (native to T1, T1 to subject, subject to group, and group to MNI) and applied to the tensor image with linear interpolation in the log space in ANTs (**c**). All warps were combined, and the combined transform was used to reorient the deformed tensor image. Maps of fractional anisotropy (FA), mean diffusivity (MD), axial diffusivity (AD), and radial diffusivity (RD) were computed on the reoriented tensor images. The FA map of the same participant is shown in **d**. These maps were analyzed with voxel-wise analyses

(PA) (Andersson et al. 2003; Andersson and Sotiropoulos 2016; Skare and Bammer 2010; Smith et al. 2004; Tournier et al. 2019). The gradient scheme containing gradient vectors and b values (b_{vecs} and b_{vals}) is stored in the header of the MRtrix file format (mif) and automatically reoriented by MRtrix functions. b_{vecs} and b_{vals} were extracted from the preprocessed image before the next step, which requires the NIFTI format. Bias field correction was performed using the N4 algorithm of ANTs (3.0) within a mask computed using the brain extraction tool (bet) of FSL on the $b=0$ preprocessed volume (Tustison et al. 2010). A brain extraction of all DWI volumes was then applied using the $b=0$ mask to remove all non-brain voxels. Preprocessed DWI volumes were smoothed anisotropically, a method in which kernels are shaped based on the main directions of fiber tracts, using the 3danisosmooth function in AFNI (19.0.26 'Tiberius') (two iterations, $\sigma_1=0.5$, $\sigma_2=1.0$) (Ding et al. 2005). This type of smoothing has been shown to preserve directional information, maintaining WM structure boundaries and limiting partial voluming effects (Van Hecke et al. 2010). This method was also shown to decrease the influence of smoothing parameters, such as kernel size, on voxel-based analysis results (Jones et al. 2005; Moraschi et al. 2010; Van Hecke et al. 2010).

DWI data were fitted to a tensor model with dwi2tensor (MRtrix 3.0) and the tensor images were converted to a symmetric matrix in the NIFTI format in the lower-triangular ordering (dxx, dxy, dyy, dxz, dyz, dzz) for ANTs. Spatial normalization was performed in ANTs using high-dimensional non-rigid registration of the tensor images, which uses both spatial and directional tensor information, and was shown to improve alignment of WM tracts and minimize shape confounds on FA outcomes (Zhang et al. 2007). Warps were computed at four levels: first, using rigid and affine transforms (with mutual information; MI, as similarity metric) to compute the warp from DWI (using the $b=0$ volume which has the highest contrast) to anatomical space (UNI image from the MP2RAGE T1 acquired in the same session), and then from anatomical (1 day) to subject space (across days), from subject to group space, and lastly to MNI space (MNI152) using rigid (MI), affine (MI), and SyN (symmetric normalization; with cross-correlation) transforms with the antsRegistration function (Avants et al. 2008, 2009). The first step of the registration process of tensor images takes care of the spatial alignment: all warps were applied to the tensor images in a single step, using antsApplyTransforms. Linear interpolation in the log space was used and, since the log of 0 is undefined, the background tensor value was set to 0.0007 (Arsigny et al. 2006). All warps were then combined, and the combined transform was used to reorient the deformed tensor images (ReorientTensor), accounting for the orientational aspect of normalization (Zhang et al. 2007). Maps of fractional anisotropy (FA), mean diffusivity (MD), axial diffusivity (AD), and radial diffusivity (RD) were then computed on the reoriented tensor images (in MNI space) using ImageMath in ANTs. A WM mask was created from the mean FA image thresholded at 0.35 to include only WM voxels in statistical analyses. All preprocessing steps of the DWI data are illustrated in Fig. 2.

Rs-fMRI data were corrected for motion and for magnetic field inhomogeneities using the acquired fieldmaps. Nuisance regression, including 12 motion regressors (three translations and three rotations plus their first derivatives), outlier regressors and physiological regressors, was performed using Nilearn's NiftiMasker. A Gaussian smoothing kernel of 2.4 mm was then applied before calculating voxel-wise network centrality metrics degree centrality (DC) and Eigenvector centrality (EC) (Wink et al. 2012). DC and EC maps were non-linearly registered to MNI space with ANTs (Avants et al. 2009). DC and EC provide a measure of the degree of connectivity of a node to other nodes, with each grey matter voxel representing a node. All preprocessing, tissue segmentation and registration scripts, which were implemented in the CBS Tools environment, are openly available at https://github.com/AthSchmidt/MMPI/tree/master/preprocessing. Preprocessing of rs-fMRI data is explained in more details in Jaeger et al. (2021).

Statistical analyses

Performance improvement in the SPFT

Performance and improvements in performance over the course of the training sessions were quantified using a measure of temporal synchronization (SYN) calculated using custom-built scripts in MATLAB (Version R2016a, The MathWorks, Inc., Natick, Massachusetts, United States). SYN was defined as the temporal deviation (in ms) between the time of the movement of the REF bar and the time when the FOR bar matches the height of the REF bar most closely. The time of best match between the REF and FOR patterns was determined using cross-correlation. The time difference (SYN in ms) was then calculated between the time of movement of the REF bar and the time lag with the greatest cross-correlation (i.e., representing the best match between REF and FOR patterns). A SYN score of zero thus indicated perfectly timed performance.

SYN score values of the three trials of each block were averaged for each participant, resulting in three block values per day. Block SYN scores were then averaged, yielding one SYN value per day. A repeated-measures ANOVA was conducted in Jamovi (https://www.jamovi.org; https://cran.r-project.org/; Lenth et al. 2018; Singmann et al. 2018), to assess the progression in performance, with Group-Task (LRN group-LRN task, LRN group-SMP task and SMP group-SMP task) as a between-subject factor and Day (1–5

and 17) as the repeated-measures factor. Mauchly's tests were conducted to assess sphericity and the appropriate correction was applied if sphericity was violated (Greenhouse–Geisser if $\varepsilon < 0.75$ or Huynh Feldt if $\varepsilon > 0.75$). Post hoc Tukey's tests were then used to assess the specific temporal location of differences in significant effects and interactions (i.e., between which days the improvement in SYN score was significant).

WM microstructural changes across learning stages

We conducted voxel-wise analyses within a WM mask on all diffusion maps (FA, MD, AD, and RD) using a flexible factorial design for longitudinal data from the CAT12 (Computational Anatomy Toolbox: http://www.neuro.uni-jena.de/cat/) in SPM12 (Statistical Parametric Mapping software: http://www.fil.ion.ucl.ac.uk/spm/) implemented in MATLAB (Version R2019a, The MathWorks, Inc., Natick, Massachusetts, United States). The flexible factorial design accounts for dependency between time points for each participant, and included two factors: Group (LRN and SMP) and Scan (d1, d2, and d5). Based on the MSL literature, putative changes between d1 and d2 were interpreted as occurring during the initial fast learning stage, d2–d5 as the subsequent slow learning stage, and d1–d5 as overall learning. The contrasts assessed were the interaction between Group and Scan in the following manner: d2 > d1, d2 < d1, d5 > d2, d5 < d2, d5 > d1, and d5 < d1. These contrasts were assessed in both groups, only within the LRN group, and with the opposite direction of change in the LRN vs SMP group (e.g., d2 > d1 in LRN, d2 < d1 in SMP), which resulted in a total of 18 contrasts. Results are reported using cluster inference with the SPM default threshold of $p < 0.001$ and FWE correction for multiple comparisons at the cluster level ($p < 0.05$). All analyses were conducted within the WM mask. We defined sequence-specific changes as significant changes in the contrasts of opposite directions between groups, where the LRN group was driving the interaction (i.e., greater change in LRN). Significant changes in both groups were defined as non-sequence specific and interpreted as related to motor execution of the SPFT. Similar voxel-wise interaction analyses were conducted on rs-fMRI centrality metrics with Group and Scan as factors, allowing to identify clusters of changes in functional connectivity (Jaeger et al. 2021), which were used for ROI generation.

WM microstructural changes associated with functional changes

Work from our group focusing on the rs-fMRI data in the same cohort identified functional reorganization of the networks involved in MSL (Jaeger et al. 2021). These regions were used to define ROIs in WM tracts associated with these task-relevant functional changes. Specifically, increases in centrality (DC and EC) were found in the right globus pallidus internal segment (GPi) in the initial learning stage (d1–d2) and bilaterally in the superior parietal cortex (SPC) in overall learning (d1–d5). Decreases in the right supplementary area (R SMA) and right pars opercularis (R PO) were also observed between d1–d5 in the LRN group. To relate structural changes in WM to functional changes, ROIs (Fig. 3, in blue) were generated from the rs-fMRI clusters in grey matter (Fig. 3, in red) using the 3dROIMaker function in AFNI (Taylor and Saad 2013). The GM ROI was first inflated by two voxels to find where it overlapped WM (within our group WM mask) and then inflated by four voxels to define an ROI within the WM. Inflating parameters were adjusted when creating the R GPi and the R SPC ROIs, to yield ROIs of similar sizes, as these clusters were located closer to the WM mask. Resulting ROIs contained 79, 187, 238, 161, and 69 voxels for the R GPi, L SPC, R SPC, R SMA and R PO, respectively. We extracted mean values from each ROI and conducted repeated-measures ANOVAs across timepoints (d1, d2, and d5) in the LRN group, with separate analyses for each diffusion metric (FA, MD, RD and AD) and ROI. Post hoc Tukey's tests were then conducted on significant effects and interactions to determine the locations of significant changes in WM metrics (i.e., between which days). These analyses focused on participants of the LRN group since ROIs from the rs-fMRI data come from an interaction analysis between groups which showed changes specific to the LRN in these regions.

Retention of WM microstructural changes

To assess whether WM microstructural changes were maintained through the retention period, paired *t* tests were conducted between mean values at d5 and those at d17 in clusters where significant changes were found during the training period (d1–d5). ROIs used for these analyses consisted in any cluster where a significant change was found with whole-brain voxel-wise analyses, as well as ROIs created from rs-fMRI clusters in which a significant change in WM microstructure was found with repeated-measures ANOVAs. These analyses focused on the LRN group and on the metrics (i.e., FA, MD, RD, or AD) that showed significant changes during the training period. A lack of significant change between mean values at d5 and those at d17 was interpreted as WM microstructural change retention.

Correlation with improvements in performance

Changes in WM metrics were correlated with performance improvements in the initial learning stage (d1–d2) and in overall learning (d1–d5). The slow learning phase (d2–d5) was not assessed since there were no significant behavioural

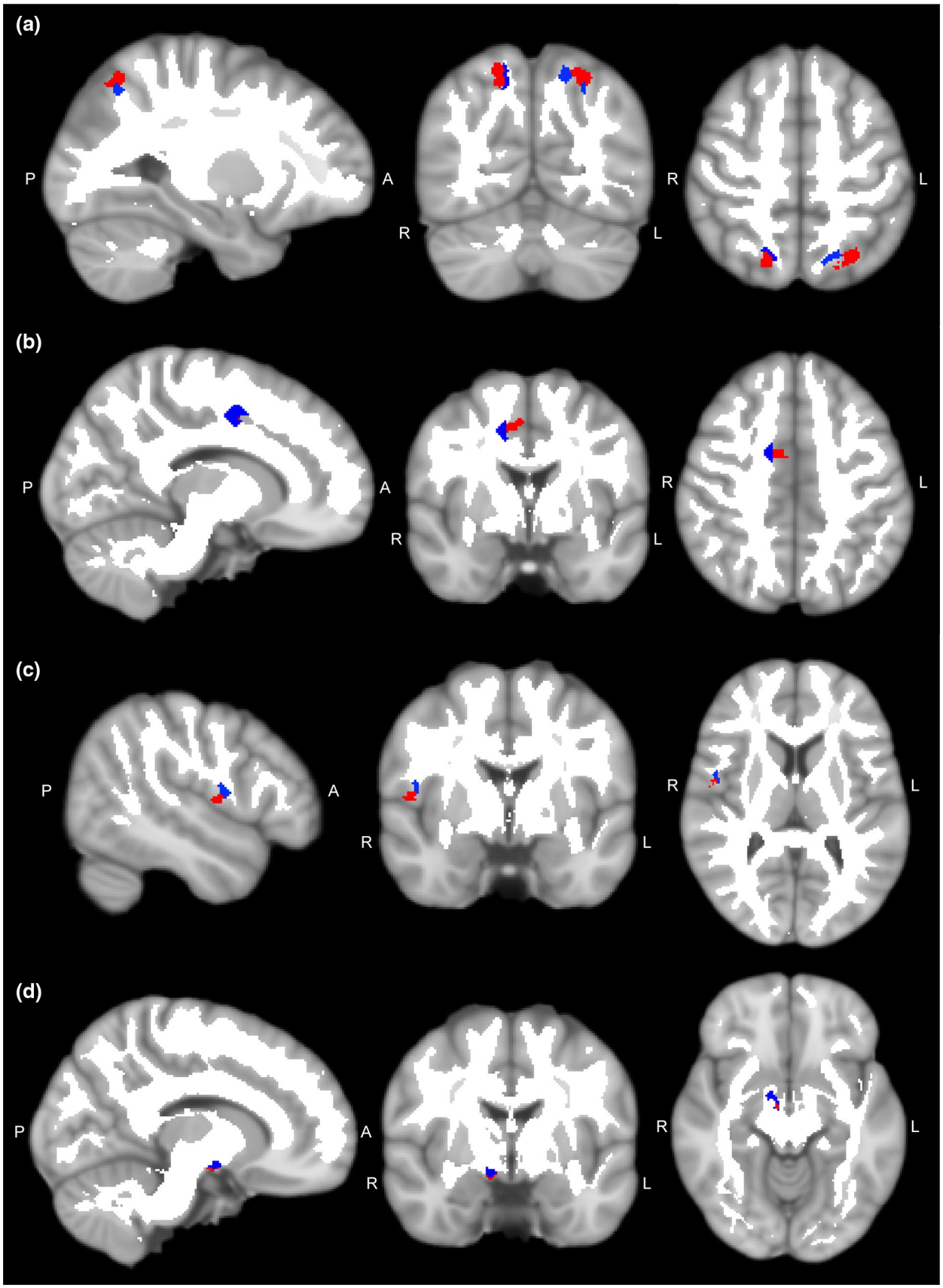
(a)
P
A
R
R
L
(b)
P
A
R
R
L
(c)
P
A
R
R
L
(d)
P
A
R
R
L

◂**Fig. 3** Regions of interest (ROIs) in white matter (blue) created from grey matter ROIs (red) where sequence-specific changes in functional connectivity were found (Jaeger et al. 2021). ROIs are displayed on the MNI152 template and WM ROIs are overlaid on a white matter mask created from the group average of FA maps thresholded at 0.35. **a** Right and left superior parietal cortex (SPC) ROIs. **b** Right supplementary motor area (SMA) ROI. **c** Right pars opercularis (PO) ROI. **d** Right globus pallidus internal segment (GPi) ROI

or structural changes during this time period. Improvements in performance were expressed as a relative change from baseline in percent to account for different baseline performance levels (i.e., SYN score at the beginning of d1) across subjects. Relative improvements in SYN (%) were calculated as: [ABS(SYNd2 − SYNd1)/SYNd1] × 100 for initial fast learning and as: [ABS(SYNd5 − SYNd1)/SYNd1] × 100 for overall improvement. These analyses aimed at investigating whether the extent of changes in WM metrics during each learning stage was related to the improvements on the task during the same period.

Results

Performance improvement in the SPFT

Participants in the LRN group learned the complex sequence progressively over the course of the training period as evidenced by the large decrease in temporal deviation (SYN) between the beginning of training (d1 block 1 mean SYN score = 224.01 ± 68.53) and the last block of d5 (89.31 ± 62.67). Moreover, the mean SYN score at the retention session (d17; 109 ± 60.5 ms) indicates that gains in performance were maintained. On the other hand, participants in the control group improved very minimally in performing the SMP task as the sequence was fairly easy and temporal deviation was already minimal at the beginning of training (mean SYN score at d1 block 1 = 33.98 ± 7.31; mean SYN at last block of d5 = 19.23 ± 5.56). Scores were significantly different between groups; a repeated-measures ANOVA revealed a significant main effect of Group ($F(2, 53) = 62.0$, $p < 0.001$) and an effect size (η^2_p) of 0.700, further showing how different the sequences are (see Fig. 4). There were no significant correlation between performance in the task and sport or musical experience ($p > 0.05$).

There was also a main effect of Day ($F(5,265) = 30.2$, $p < 0.001$, $\eta^2_p = 0.363$) and a significant interaction of Day × Group ($F(5,265) = 20.7$, $p < 0.001$, $\eta^2_p = 0.438$). These main effects and interactions were still significant ($p < 0.001$) after Greenhouse–Geisser correction which was applied because sphericity was violated in this analysis. Consistent with the theories of learning stages, most improvements took place in the first days and then reached a plateau at d4 in the LRN group performing the complex task (LRN); post hoc Tukey was significant between d1 and d2 ($t = 7.864$, $p < 0.001$), d2–d3 ($t = 4.367$, $p = 0.002$), and nearly significant d3–d4 ($t = 3.497$, $p = 0.054$), but not significant between d4 and d5 ($t = -0.774$, $p = 1.000$), nor between d5 and d17 ($t = -1.755$, $p = 0.953$) (Fig. 4). Post hoc Tukey was also significant between d1–d17 ($t = 13.199$, $p < 0.001$) and d2–d17 ($t = 5.335$, $p < 0.001$), but not between d5 and d17 ($t = -1.755$, $p = 0.953$) indicating that performance in the task was maintained after 12 days without practice.

In contrast, participants in the SMP group exhibited little significant improvement over the course of the 5 days of training. None of the pairwise comparisons between consecutive days were significant in this group and Post hoc Tukey was also non-significant between d1 and d5, indicating no significant improvement in the overall learning period. There was no significant difference between the performance of the LRN group and that of the SMP group on the SMP task (post hoc Tukey $p > 0.05$ between LRN group-SMP task and SMP group-SMP task at every time point). As expected, SYN scores of both groups performing the SMP task differed significantly from the SYN scores of the LRN task (post hoc $p < 0.001$ at every time point). Two participants from the SMP group were excluded from the analysis because their SYN scores on d3, and d4 for one of them, were outliers as they exceeded the mean by more than two SD.

WM microstructural changes across learning stages

Changes of opposite directions in both groups were found in the corticospinal tract, underlying the left primary motor cortex (M1) ($t = 4.20$, $p = 0.002$; Fig. 5b). FA decreased in LRN, whereas FA increased in this cluster in SMP (d5 < d1 in LRN, d5 > d1 in SMP). The mean ΔFA in LRN was − 0.029, while FA increased by 0.0395 in the SMP group. Voxel-wise analyses also revealed a decrease in FA ($t = 5.01$, $p = 0.005$; mean ΔFA = − 0.176) in the right ascending sensorimotor tract adjacent to the primary somatosensory cortex (S1), in the LRN group only, during overall learning (d5 < d1; see Fig. 5a). Other DTI metrics for these contrasts were non-significant ($p_{FWE} > 0.05$).

There were also changes in FA in the same regions in both groups. These plastic changes were common to both groups and therefore considered non-sequence specific and more related to motor execution. FA had a near significant increase in the frontal inferior longitudinal (FIL) tract underlying the right pars opercularis (PO) in the early stage of learning (d2 < d1; Fig. 5c) in both groups ($t = 4.02$, $p = 0.063$; mean ΔFA in all subjects = 0.115, mean ΔFA in LRN = 0.125, mean ΔFA in SMP = 0.104). In overall learning, FA increased significantly in the right anterior corona radiata adjacent to the frontal eye field (FEF; $t = 5.28$, $p = 0.023$; Fig. 5d) in both groups (mean ΔFA in all subjects = 0.119, mean ΔFA in LRN = 0.147,

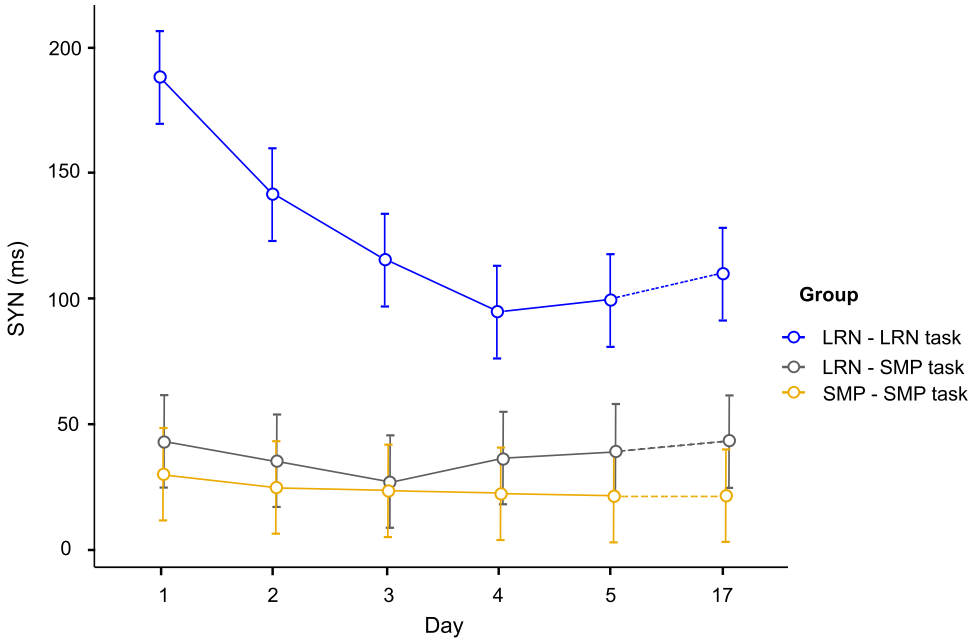

Fig. 4 Behavioral results. Temporal deviation (SYN; in ms) for each group and each task across training days (d1–d5) and retention session (d17), where the SYN value of each day is the mean across blocks. LRN–LRN task: learning group performing the LRN task (in blue); SMP–SMP task: control group performing the SMP task (in orange); LRN–SMP task: learning group performing the SMP task (in grey). Error bars represent the standard error of the mean

mean ΔFA in SMP = 0.093). Other metrics for these contrasts, and all other contrasts assessed, were non-significant ($p_{FWE} > 0.05$). The results are summarized in Table 2.

WM microstructural changes associated with functional changes

WM microstructure in the ROI underlying the right SMA was altered during the training period in the LRN group (Fig. 6a). FA was found to decrease significantly across days ($F(2, 36) = 5.82$, $p = 0.006$, $\eta^2_p = 0.244$; Fig. 6b) and Tukey's post hoc test revealed that this decrease was significant between d1 and d2 ($t = 3.072$, $p = 0.011$) and between d1 and d5 ($t = 2.823$, $p = 0.021$), but not between d2 and d5 ($t = -0.249$, $p = 0.966$). There was also a significant decrease in AD (Fig. 6c) in the R SMA ($F(1.38, 24.91) = 6.27$, $p = 0.012$ after Greenhouse–Geisser correction, $\eta^2_p = 0.258$) and post hoc tests showed that the differences were statistically significant between d1 and d2 ($t = 3.300$, $p = 0.006$) and between d1 and d5 ($t = 2.763$, $p = 0.024$). RD increased significantly across days ($F(1.44, 25.99) = 3.93$, $p = 0.044$ after Greenhouse–Geisser correction, $\eta^2_p = 0.179$) (Fig. 6d). This increase bordered on statistical significance in post hoc Tukey's tests between d1 and d2 ($t = -2.419$, $p = 0.053$) and between d1 and d5 ($t = -2.438$, $p = 0.051$), but not between d2 and d5 ($t = -0.0190$, $p = 1.000$). MD showed no significant change in this ROI ($p > 0.05$). To test whether the DTI metrics changed in the SMP group, the same analyses (RM-ANOVAs) were conducted in that group. Diffusion metrics did not change significantly across days in the SMA ROI in the SMP group ($p > 0.05$).

Diffusion metrics in the other ROIs (L and R SPC, R GPi, and R PO) did not change significantly across days in repeated-measures ANOVA analyses.

Retention of WM microstructural changes

Changes in FA in the right S1 and left M1, which both decreased significantly between d1 and d5 in LRNs, were not maintained at the retention session (d17). Paired samples *t* tests revealed significant differences between mean FA values at d5 and mean FA at d17 (S1: $t(18) = 2.25$, $p = 0.037$; M1: $t(18) = 2.94$, $p = 0.009$) in the LRN group. There was, however, no significant difference between mean FA at d5 and at d17 in the WM tract underlying the left M1 in the SMP group ($t(19) = 1.11$, $p = 0.279$). Refer to Supplemental Fig. 1 for the time course of FA changes in S1 and M1.

FA in the right PO was not significantly different between d5 and d17 ($t(38) = -1.31$, $p = 0.197$). However, when inspecting the time course of changes relative to baseline (see Supplemental Fig. 1), we can see that FA slowly decreases after the time point of significant change (d1–d2; in both groups), from d2 to d17. Retention did not take place in the right FEF, where FA, which increased across the overall training period (d1–d5) in both groups, then decreased significantly between d5 and d17 ($t(38) = -2.93$, $p = 0.006$).

Changes in all WM metrics were maintained at d17 in the right SMA (Fig. 6). There were no significant differences between the mean values at d5 and those at d17 for FA and AD, which both decreased in the early stage of training (d1–d2) in the LRN group (FA: $t(18) = 0.035$, $p = 0.972$;

AD: $t(18) = -0.174$, $p = 0.863$). The increased RD was also maintained at d17 as evidenced by the non-significant t test d5–d17 ($t(18) = 0.025$, $p = 0.981$).

Correlation with improvements in performance

No significant correlation between changes in FA and improvement in performance was found ($p > 0.05$).

Discussion

In this study, we investigated structural changes in WM over the course of five training days on a continuous visuomotor sequence task using DTI. Consistent with the behavioral results, where the greatest amount of improvements in temporal synchronization (SYN) were detected between the two first days (see Fig. 4), we observed structural changes in WM only in the early phase of learning (d1–d2), and when looking at the overall learning period (d1–d5), which suggests a slower, more progressive change. Sequence-specificity was assessed through interaction analyses between the LRN group, who performed a complex sequence, and the control group (SMP), who performed a simple sequence, where the interaction is driven by the LRNs. FA was found to change in opposite directions in both groups in the left corticospinal tract (CST) inferior to the primary motor cortex (M1; Fig. 5b) during overall learning. However, as the SMP group showed a greater change than the LRNs, we cannot establish that altered FA in WM underlying M1 is due to sequence learning per se. Changes in the right ascending sensorimotor tract (SMT) adjacent to the primary somatosensory cortex (S1) were also observed in the LRN group (Fig. 5a). Changes underlying M1 and S1 were, however, not maintained at the retention session, 12 days after cessation of training. WM microstructure was altered during the early phase of learning in the ROI underlying the right supplementary motor area (SMA; Fig. 6), where sequence-specific changes in functional connectivity were found during overall learning in this cohort (Jaeger et al. 2021). Changes in WM microstructure underlying the right SMA were maintained at the retention session. Together, our findings provide evidence for training-dependent white matter plasticity in the sensorimotor network during short-term motor sequence learning.

Changes in the LRN group

Overall learning—right primary somatosensory cortex (S1)

Fractional anisotropy decreased in the right ascending SMT in participants of the LRN group during overall learning (d1–d5; Fig. 5a). We hypothesize that this decrease in FA in fiber tracts connecting to the right S1 may reflect suppression of activity in S1 ipsilateral to the hand used in the SPFT (Kastrup et al. 2008; Staines et al. 2002). Increased activity in the contralateral S1, and suppression of activity in the ipsilateral S1, as a result of task-relevant somatosensory stimulation and voluntary movements, have been reported in fMRI and EEG studies (Kastrup et al. 2008; Lei and Perez 2017; Nirkko et al. 2001; Staines et al. 2002). Blood flow suppression along with inhibition of S1 areas that are not involved in a task (e.g., ipsilateral body parts) from the prefrontal-thalamic system have been suggested as mechanisms to selectively gate sensory inputs (Drevets et al. 1995; Knight et al. 1999; Staines et al. 2002; Yamaguchi and Knight 1990). In work by Drevets et al. (1995), blood flow reductions were observed in S1 ipsilateral to the expected stimulus when participants were anticipating somatosensory stimulation. The fact that changes in the SMT were only found in the LRN group may be due to increased levels of anticipation and attention in participants performing a complex task (Drevets et al. 1995; Halsband and Lange 2006; Staines et al. 2002). We speculated that the increased attention necessary to perform the complex task would likely require greater activation of the dorsolateral prefrontal cortex. This could lead to greater inhibition of the ipsilateral S1, through the prefrontal-thalamic sensory gating system, as a way to suppress background noise and enhance processing of task-relevant inputs (Corbetta and Shulman 2002; Halsband and Lange 2006; Staines et al. 2002; Yamaguchi and Knight 1990). Participants of the SMP group on the other hand may not need to pay as much attention to the task at hand, and to the associated sensory inputs, and may perform the repetitive sinusoidal sequence in a more automated manner.

This sensory gating, in which behaviorally irrelevant regions are inhibited to effectively suppress unimportant, and potentially disruptive, inputs, may thus contribute to enhancing the responsiveness of the contralateral S1 to stimuli (Staines et al. 2002). Enhanced somatosensory inputs while performing a motor task have been associated with improvements in performance, and disrupting somatosensation during training impairs motor learning (Vidoni et al. 2010; Wei et al. 2018). As participants in this study were holding a pressure sensor between their thumb and index fingers, enhanced somatosensory inputs to the central nervous system due to SPFT training could result in the acquisition of a new task-specific sensory map (Braun et al. 2000; Pascual-Leone et al. 2005). This would provide better sensory feedback when subsequently performing the task, which could translate into improved accuracy in matching the reference bar (Wei et al. 2018).

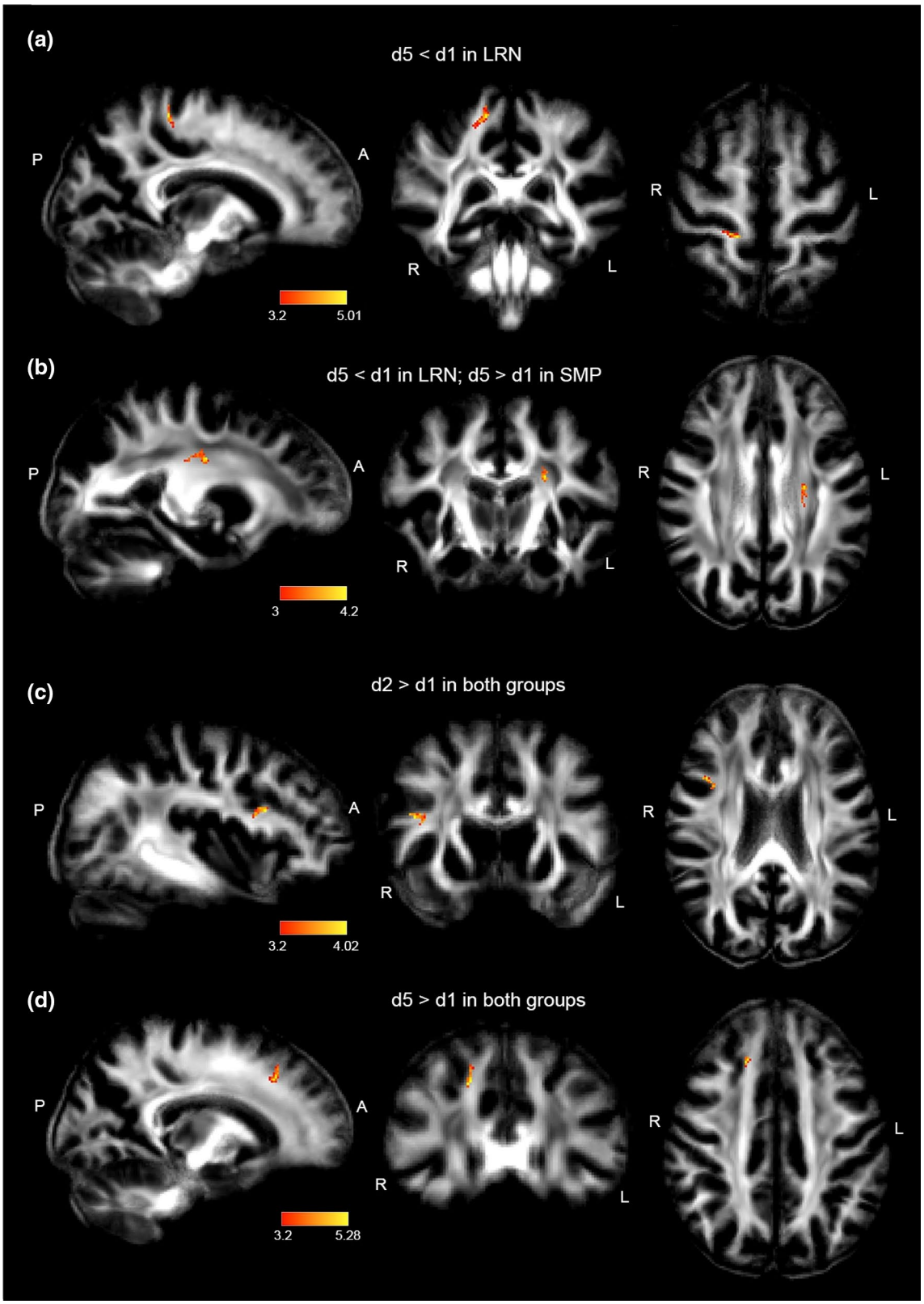
(a)
d5 < d1 in LRN
P
A
R
L
R
L
3.2
5.01
(b)
d5 < d1 in LRN; d5 > d1 in SMP
P
A
R
L
R
L
3
4.2
(c)
d2 > d1 in both groups
P
A
R
L
R
L
3.2
4.02
(d)
d5 > d1 in both groups
P
A
R
L
R
L
3.2
5.28

◂**Fig. 5** Changes in FA from voxel-wise analyses. T-stat maps (maximum intensity projection for better visualization) are overlaid on the mean FA image. **a** Decrease in FA in the LRN group between d1 and d5 in the right ascending sensorimotor tract connecting to the primary somatosensory cortex (S1). **b** Decrease in FA in LRN and increase in FA in SMP between d1–d5 in the left corticospinal tract connecting to the primary motor cortex (M1). **c** Increase in FA in both groups between d1 and d2 in the right frontal inferior longitudinal (FIL) tract connecting to the pars opercularis (PO). **d** Increase in FA in both groups between d1 and d5 in anterior corona radiata connecting to the right frontal eye field (FEF)

Overall learning—left primary motor cortex (M1)

FA in the left CST connecting to M1 was found to decrease in the LRN group, while it increased in the SMP group during overall learning (d1–d5; Fig. 5b), indicating a relatively slow change in this region over the course of the five training days. As the SMP group did not show any significant improvement in the SPFT, we are cautious in interpreting a change in this group without supporting behavioral evidence. The change in the LRN group on the other hand was accompanied by a change in behavior. We will thus focus the interpretation on the LRN group although we could speculate that any plastic change occurring in the SMP group could mirror changes in the LRNs but occur on a shorter time scale, as the sequences learned by each group have different complexities (Dayan and Cohen 2011; Hyde et al. 2009; Karni et al. 1995).

Since we expect M1 to be activated when performing a motor task with the contralateral limb, as M1 has a known role in motor execution and the storage of learned sequence representations (Bengtsson et al. 2005; Hardwick et al. 2013; Hyde et al. 2009; Monfils et al. 2005; Penhune and Steele 2012; Yokoi et al. 2018), this decrease in FA in the group performing a more complex task may seem contradictory. However, activity in M1 was previously shown to progressively decrease as a motor skill is learned (Dayan and Cohen 2011; Poldrack 2000; Seidler et al. 2005), possibly reflecting increased efficiency. Moreover, functional connectivity in M1 was found to increase in the LRN group during the early stage of training (Jaeger et al. 2021). This suggests an important and active role of this area as we begin to learn a task, but then, as the motor sequence is learned, less neuronal resources would be needed to perform the task which could be reflected by decreased connectivity (Dayan and Cohen 2011; Poldrack 2000). In line with this, studies in musicians, experts in sensorimotor control, have also reported lower FA in motor circuits, including the bilateral CST and corona radiata (Imfeld et al. 2009; Penhune and Steele 2012 for review; Schmithorst and Wilke 2002). This decrease in anisotropy may be due to increased efficiency, or it may result from changes in the permeability of axonal membranes to water, or to an increased axonal diameter, which would lead to an increase in intracellular radial diffusivity (Beaulieu 2002; Imfeld et al. 2009; Zatorre et al. 2012). Lastly, the development of a secondary fiber population in areas of crossing fibers is another potential mechanism through which FA could be reduced (Zatorre et al. 2012). Indeed, another study investigating structural changes associated with 5 days of MSL found that lower FA in the CST on the last training day correlated with better performance on the task (Steele et al. 2012). Since the significant correlation was located in a region where the CST and superior longitudinal fasciculus (SLF) cross, they hypothesized that maturation of the SLF, which would be the secondary fiber population here, drove the reduction in FA and promoted performance, as the SLF connects cortical regions that are involved in this task. The lack of significant changes in other diffusivity metrics in this study, however, does not allow to disentangle the extent to which these factors contribute to the reduction in FA observed in the CST. Acquiring a greater number of diffusion gradient directions and strengths, and using more advanced diffusion models such as neurite orientation dispersion and density imaging (NODDI), and tractography, may allow to distinguish the underlying factors leading to altered FA in future studies (Steele and Zatorre 2018; Tardif et al. 2016; Zhang et al. 2012). However, the increase in functional connectivity observed during the early stage of learning (Jaeger et al. 2021), along with the slower decrease in FA found in this study, support the hypothesis of a strong initial M1 involvement, followed by decreased M1 activation as learning progresses, reflecting enhanced network efficiency (Bassett et al. 2015; Costa et al. 2004; Dayan and Cohen 2011; Finc et al. 2020; Karni et al. 1995; Mohr et al. 2016; Poldrack 2000).

Fast learning—right supplementary motor area (SMA)

ROI-based analyses were conducted in WM tracts underlying clusters of changes in resting-state centrality metrics, which included bilateral SPC, right GPi, right SMA and right PO (inferior part) (Fig. 3). These analyses revealed changes in the WM ROI underlying the right SMA, in a fiber pathway we identified as the frontal aslant tract (FAT) (Fig. 6a). The FAT connects the superior frontal gyrus (SFG), including the supplementary motor area (SMA), to the IFG (Briggs et al. 2018) and is thought to have a role in working memory, motor planning and coordination (Dick et al. 2019; Varriano et al. 2020). This pathway may function to coordinate sequential motor movements, especially in visuo-spatial tasks, to select the appropriate motor outputs (Dick et al. 2019). Moreover, the SMA has been shown to be involved in long-term (Hikosaka et al. 1995, 1996; Jenkins et al. 1994; Shima and Tanji 2000; Tanji 1996; van Mier et al. 1998), and short-term MSL (Vollmann et al. 2013), especially in action planning and

Table 2 Clusters in which significant changes in FA were found

	k (#voxels)	p_{FWE}	T	Peak coordinates in MNI (mm)	Region
d5 < d1 in LRN	38	0.005	5.01	[14, − 35, 60]	R ascending sensorimotor tract adjacent to S1 (Fig. 5a)
d5 < d1 in LRN; d5 > d1 in SMP	42	0.002	4.20	[− 24, − 11, 30]	L corticospinal tract adjacent to M1 (Fig. 5b)
d2 > d1 in both groups	25	0.063	4.02	[41, 14, 23]	R frontal inferior longitudinal tract adjacent to PO (Fig. 5c)
d5 > d1 in both groups	30	0.023	5.28	[17, 29, 41]	R anterior corona radiata adjacent to FEF (Fig. 5d)

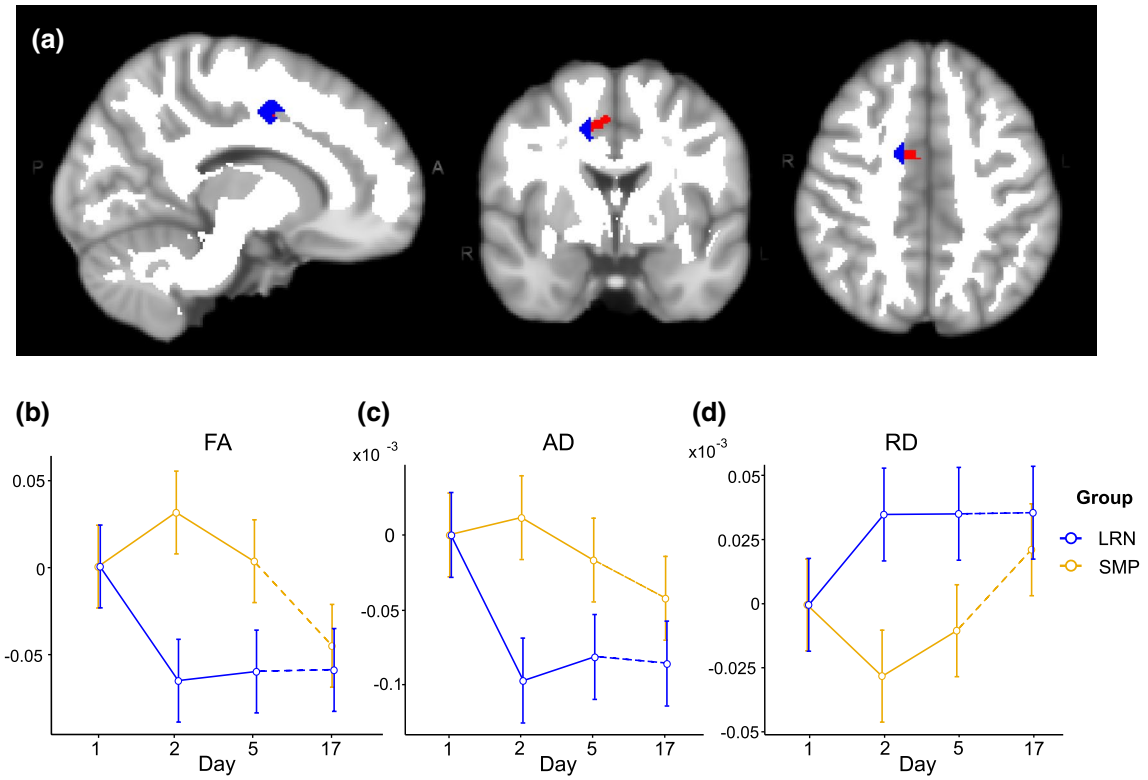

Fig. 6 Changes in WM microstructure in the ROI underlying the right supplementary area (SMA) in which sequence-specific changes in functional connectivity were found (Jaeger et al. 2021). **a** The right SMA ROI from resting-state analyses (in red) and the WM ROI (in blue; overlaid on the WM mask in white) are both overlaid on the MNI152 template. Mean change in DTI metrics from baseline (d1) in both groups: **b**, **c** FA and AD decreased in the LRN group (blue lines) between d1 and d2 and remained lower at d5 and d17. **d** RD increased between d1 and d2 in LRN and remained higher at d5 and d17. DTI metrics in the right SMA in the SMP group did not change significantly ($p > 0.05$). Error bars represent the standard error of the mean

in the organization of temporal aspects, such as timing and order, in a wide range of domains (e.g., language, working memory, motor sequences) (Cona and Semenza 2017; Krakauer et al. 2019). A study using the same task provided strong evidence of the implication of the SMA in sequence learning by showing that non-invasive stimulation over the SMA led to improvements in performance of the SPFT (Vollmann et al. 2013).

Considering the known role of the SMA and FAT in sequence processing (Cona and Semenza 2017; Dick et al. 2019; Krakauer et al. 2019; Shima and Tanji 2000; Tanji 1996; Varriano et al. 2020; Vollmann et al. 2013), we may expect connectivity to be enhanced with this type of task. However, work from our group has found decreases in functional connectivity in the right SMA and right PO during overall learning in the same cohort (Jaeger et al. 2021). It was hypothesized that reduced connectivity in these regions may thus reflect increased efficiency, or decreased need for resources to plan and coordinate movements, which would result in segregation of the network. This hypothesis is consistent with the view that the integration of multiple large-scale networks is necessary in the early stages of learning (Finc et al. 2020) and then, as a skill is mastered and becomes nearly automatic, a more easily reachable network,

consisting in autonomous segregated modules, is sufficient to execute the task (Bassett et al. 2015; Finc et al. 2020; Mohr et al. 2016). In the present study, we found decreases in FA and AD in the WM ROI underlying the right SMA in the LRN group, during the early stage of learning and in overall learning, which were maintained during the retention period (Fig. 6a–c). These findings, along with the increase in RD during the same period (Fig. 6d), suggest a decrease in structural connectivity in the right SMA, which precedes a reduction in functional connectivity in the same region (Jaeger et al. 2021). The idea of structure preceding function may seem contradictory; however, resting-state connectivity is not assessed online, during task performance. Since WM tracts form the structural basis of connectivity, linking regions within resting-state networks, modulation of the supporting connections may be necessary to allow for greater communication. We could thus hypothesize that WM microstructure is altered in response to increased or decreased activation in a region during task performance (online) (Day and Sweatt 2011; Fields 2015; Forbes and Gallo 2017; Zatorre et al. 2012) and that this then leads to modulations of resting-state networks (offline; rs-fMRI). It is therefore possible that structural changes underlie the subsequent changes in functional connectivity, though future studies would be necessary to fully investigate this hypothesis.

The spatial and temporal patterns of WM structural changes observed in the current study are in line with a theoretical framework describing two networks operating in parallel during MSL with different time courses (Hikosaka et al. 2002). Those two networks would each subserve distinct aspects of MSL: learning spatial coordinates, supported by a prefronto-parietal loop, and learning motor coordinates, which occurs more slowly and is supported by a M1-sensorimotor loop (Dayan and Cohen 2011; Hikosaka et al. 2002). Both of these loops also receive contributions from different parts of the striatum and cerebellum depending on the learning stage and on the component learned (spatial vs motor) (Hikosaka et al. 2002; Penhune and Steele 2012). Interestingly, we observed changes only in the motor loop (M1 and S1). This may be due to the fact that learning spatial coordinates requires less time than learning motor coordinates (Hikosaka et al. 2002; Miller and Cohen 2001; Penhune and Steele 2012). This could mean, in the context of the SPFT, that spatial learning took place within the first session, perhaps on the timescale of minutes or hours considering the low complexity of the spatial coordinates to be learned in this task, and did not induce changes in WM that we could detect considering the much longer timescale of our measurements (i.e., days). Moreover, as a sequence is learned, its performance becomes more implicit, and thus relies more heavily on motor mechanisms and very little on attention-demanding spatial mechanisms (Hikosaka et al. 2002; Penhune and Steele 2012). The SMA, another area in which we observed changes, both functionally (Jaeger et al. 2021) and structurally, would provide the link between those two parallel loops, allowing for updated spatial representations to be used by the M1-sensorimotor loop to optimize motor output, according to this framework (Hikosaka et al. 2002). Indeed, Penhune and Steele (2012) emphasized the need for a high degree of interaction between these parallel systems to optimize MSL. The time course of changes in WM tracts underlying the SMA (fast change; d1–d2), and S1-M1 (slower changes; d1–d5), is also in line with the hypothesis that the SMA is involved in converting quickly acquired spatial coordinates to motor coordinates which are then processed by the M1-sensorimotor loop (Hikosaka et al. 2002). Moreover, the retention of WM microstructure alterations in the fiber tracts underlying the SMA points to a lasting role of this region in sequence learning. If the SMA is indeed involved in linking spatial to motor coordinates as has been shown previously (Hikosaka et al. 2002; Penhune and Steele 2012), effectively mapping spatial representations to the appropriate motor outputs, this lasting change in underlying WM would suggest that these maps between coordinate spaces become part of long-term storage. The SMA is known for its role in sequence-specific learning and has been shown to be involved in the storage of sequence representations (Krakauer et al. 2019). The lasting changes observed in the WM tracts underlying the SMA in our study may thus reflect enhanced sequence storage efficiency in a more segregated, or autonomous, network (Bassett et al. 2015; Mohr et al. 2016).

Our findings are in line with previous literature (Bloechle et al. 2016; Karni et al. 1995; Klein et al. 2019; Lotze et al. 2003; Schmithorst and Wilke 2002; Zatorre et al. 2012) and point to the highly dynamic plastic processes in WM tracts underlying the SMA-M1-sensorimotor loop, which parallel functional changes. It has been suggested that increases in anisotropy may reflect ongoing enhancement of fibers organization while decreased FA may be related to increased network efficiency in later stages of learning (Schmithorst and Wilke 2002).

Changes in both groups

Changes in anisotropy were also observed in both groups, suggesting the involvement of a number of regions in motor execution rather than sequence-specific learning. While no change in performance common to both groups was observed, participants of both groups performed a very similar task, made up of the same movements but ordered in sequences of different complexities, on five consecutive days. The element all participants have in common is thus the execution of these pinching movements daily. We provide a putative interpretation of these results below.

FA increased in WM tracts underlying the inferior frontal gyrus (IFG; opercular part) in the early stage of training (d1–d2; Fig. 5c), and in the right anterior corona radiata (aCR) adjacent to the right frontal eye field (FEF) during overall learning (d1–d5; Fig. 5d).

Overall learning—right frontal eye field (FEF)

The frontal eye field (FEF) is involved in processing visual inputs and controlling voluntary eye movements and its activation is thought to be dependent on the saliency of the target (i.e., whether the target is behaviorally relevant) (Schall and Bichot 1998; Vernet et al. 2014). In this task, participants maintained the gaze on the computer screen where the REF and FOR bars (Fig. 1) provided both instructions (REF) and feedback (FOR) for the SPFT. Maintaining the gaze on a visual target for extended periods of time (~ 20 min/day for five consecutive days) may require high sustained activation in the FEF which could translate into structural changes in fiber tracts connecting this region during the overall learning period. The FEF clearly plays an important role in visually guided tasks, but its role has been investigated mostly in the context of goal-oriented saccadic eye movements (Schall and Bichot 1998). However, in addition to its role in target selection in saccades, the FEF is also involved in the detection and analysis of visual inputs during periods of fixation of the gaze (Posner 1980; Schall 2004; Schall and Bichot 1998). Non-invasive neurostimulation of the right FEF was shown to enhance visual perception and improve performance in a visual detection task (Chanes et al. 2012). Other studies support the idea that the FEF, especially of the right hemisphere, is involved in shifting visual attention without eye movement (Donner et al. 2000; Grosbras and Paus 2002). Moreover, the FEF may play a role in short-term memory of visuo-spatial information (Clark et al. 2012; Gaymard et al. 1999). The high potential for plasticity of the FEF has made this region a target for neurostimulation to increase visuo-spatial attention in healthy and patient populations (Vernet et al. 2014). Our results, showing FA increases in both groups, support the view that the FEF is highly plastic and suggest that this region is relevant in directing visual attention regardless of task complexity.

Fast learning—right pars opercularis (PO)

Increased FA was also observed in the frontal inferior longitudinal (FIL) tract underlying the dorsal part of the right pars opercularis (PO) between d1 and d2 (Fig. 5c). The FIL tract is a chain of u-shaped fibers connecting the dorsal part of the IFG (including the PO), to the middle frontal gyrus and precentral gyrus (M1) (Catani et al. 2012). U-fibers of the frontal and parietal lobes have been shown to play an important role in sensorimotor integration (Catani et al. 2012, 2017), and have been hypothesized to coordinate movement planning and execution by linking motor and premotor regions (Catani et al. 2012). Moreover, the right PO has been specifically linked with fine motor control of manual motion (Briggs et al. 2019; Liakakis et al. 2011).

Our findings suggest that high task complexity might not be necessary to recruit the PO and incur structural changes in the underlying WM tracts, as the SMP sequence also requires the integration of sensory information to execute the task, as well as fine motor control for the appropriate amount of force to be applied on the device at the right time. Furthermore, the change in fiber tracts underlying the PO was observed in the early stage of learning, which may indicate a greater need for sensorimotor integration at this stage.

Relationships between behavioural and WM microstructural changes

Although the fact that most improvements occurred in the initial stage of learning (d1–d2) is consistent with the time period when changes in WM microstructure were found (d1–d2 and d1–d5), the time courses of behavioural and WM microstructural changes were different. While temporal deviation (SYN) followed an exponential decay across time (i.e., improvement in performance), changes in WM appeared highly dynamic, with early changes which were maintained in some instances (i.e., SMA), as well as slow decreases in FA which were not maintained at the retention session (e.g., S1 and M1). This makes it challenging to relate behavioral to structural changes at the same time point and may explain why significant correlations were not found in this study. Other longitudinal plasticity studies have shown inconsistent relationships between brain plastic changes and behavioral outcomes with some studies reporting associations (e.g., Takeuchi et al. 2010), while others report no relationship (e.g., Scholz et al. 2009), or relationships in directions opposite to what is expected (for review, Zatorre et al. 2012). It has been suggested that correlations between performance and brain structural changes may be more closely linked to the amount of time spent training than on performance outcomes (Scholz et al. 2009). However, the fact that we did not identify a significant correlation between behavioural change and WM microstructural change is likely due to behaviour being the result of the integration of structural changes in WM and GM, as well as functional changes. Thus, WM changes alone could not predict the extent of performance improvement on the task. However, as some of the significant changes in WM were observed only in the LRN group, the only group showing behavioral change, in regions known for their role in motor sequence learning (i.e., SMA, M1, and S1), we argue that this provides evidence of behavioral relevance. Lastly, our findings showed different brain regions are involved in different stages of learning,

suggesting the SMA became involved early in learning and had a persistent role in learning the SPFT, with changes still present 12 days after cessation of training, whereas sensorimotor regions played a more transient role. A better understanding of the relationships between changes in the brain's structure and behavior would thus likely be achieved using multi-parametric models that take into account several aspects of brain plasticity to identify the most relevant parameters.

Limitations and future considerations

The main limitation of this study is that the high field strength (7 T) may make our findings less generalizable across studies, as 3 T is still much more commonly used in research. The high spatial resolution of our acquisition may have also led to a decrease in SNR. Moreover, despite the high spatial resolution of our acquisition, the angular resolution was low, with only 20 directions, and a single diffusion gradient strength was applied (i.e., one shell). The angular sampling, number of diffusion shells and gradient strength were limited due to time constraints, as the study involved the acquisition of several other MRI sequences of long duration. In future studies, DWI acquisitions with higher gradient strengths and a greater amount of directions would allow for tractography to be performed, which would increase certainty when identifying fiber tracts where changes in scalar DTI metrics are observed, and for tract-based quantification of DTI metrics (Mukherjee et al. 2008; Wakana et al. 2007). Furthermore, with a higher number of shells and directions, more advanced modelling approaches, such as NODDI, can be used, which would allow to disentangle factors such as fiber density and orientation dispersion, especially in areas of crossing fibers (Steele and Zatorre 2018; Tardif et al. 2016; Zhang et al. 2012). Furthermore, the combination of multiple quantitative MR parameters, such as magnetization transfer saturation (MTsat), proton density (PD) and longitudinal and transverse relaxation rates (R1 and R2*), would allow to specify the contributions of myelination and changes in axon morphology to training-induced WM plastic changes (Caeyenberghs et al. 2016; Deoni et al. 2008; Helms et al. 2008; Weiskopf et al. 2015).

Another challenge when investigating neuroplasticity in MSL is that high variability in the duration of each learning stage, depending on the complexity of the task, makes it difficult to relate stage-specific findings across studies (Dayan and Cohen 2011; Hyde et al. 2009; Karni et al. 1995). Moreover, our experimental design did not allow us to distinguish structural changes occurring during consolidation (i.e., offline), from those occurring during training (i.e., online). However, it is unlikely that the techniques used in the current study would have had the sensitivity to detect such subtle differences and the structural changes observed in WM are likely the sum of alterations taking place both during the training session (i.e., online) and in between sessions (i.e., offline).

Lastly, the motor sequence training period was of short duration in the present study which may limit the amount of observable structural changes. A longer training duration may have led to a greater amount of plastic changes in WM tracts which could have provided further insights into MSL-related neuroplasticity.

Conclusion

Our study provided evidence for white matter plasticity in the sensorimotor network, where the SMA plays a role in linking the spatial and motor aspects, in short-term learning of motor sequences. Our findings also highlighted the time course of plastic changes in this network as we scanned participants not only in the beginning and at the end of training, but also on the second day, allowing for the characterization of changes occurring in the early stage of training. Future ultra-high field MRI studies investigating plasticity in the context of MSL should use a high angular resolution, and a higher number of diffusion shells of varying strengths. This would provide more precision in localizing areas of change and in characterizing the biological underpinnings of plastic changes in brain white matter.

Supplementary Information The online version contains supplementary material available at https://doi.org/10.1007/s00429-021-02267-y.

Acknowledgements We would like to thank Elisabeth Wladimirov and Domenica Wilfling for their help and involvement in data acquisition and logistics of the multi-modal plasticity initiative (MMPI) dataset. This work was supported by the Max Planck Society, the MaxNetAging Research School (Max Planck Institute for Demographic Research, ATJ), the NWO Vici grant (PI: Birte Forstmann)(PLB), the National Science and Engineering Research Council (NSERC; CJG: RGPIN 2015-04665, CJS: RGPIN-2020-06812, DGECR-2020-00146), the Michal and Renata Hornstein Chair in Cardiovascular Imaging (CJG), the Heart and Stroke Foundation (New Investigator Award, CJG and CJS), the Canadian Institutes of Health Research (HNC 170723), the Fonds de Recherche du Québec—Nature et Technologies (CJS and JH), the Fonds de Recherche du Québec—Santé (JH), and the Réseau de Recherche en Santé cardiométabolique, diabète et obésité (CMDO; JH).

Author contributions All authors contributed to the study and approved the final manuscript. Detailed contributions, described according to CRediT, were as follow: conceptualization: CLT, P-LB, AV, CJS, and CJG; methodology: CLT, P-LB, CJG, and CJS; data collection: P-LB, US, SG, A-TJ, and JH; formal analysis: SAT, A-TJ, CG, and SB; software: P-LB, CJS, and JH; writing—original draft preparation: SAT; visualization: SAT; writing—review and editing: A-TJ, P-LB, CG, CJS, and CJG; funding acquisition: AV; supervision: CJS and CJG.

Funding This study was funded by the Max Planck Society, the MaxNetAging Research School (Max Planck Institute for Demographic

Research, ATJ), the NWO Vici Grant (PI: Birte Forstmann)(PLB), the National Science and Engineering Research Council (NSERC; CJG: RGPIN 2015-04665, CJS: RGPIN-2020-06812, DGECR-2020-00146), the Michal and Renata Hornstein Chair in Cardiovascular Imaging (CJG), the Heart and Stroke Foundation (New Investigator Award, CJG and CJS), the Canadian Institutes of Health Research (HNC 170723), the Fonds de Recherche du Québec—Nature et Technologies (CJS and JH), the Fonds de Recherche du Québec—Santé for the scholarship for Training course abroad (Quebec Bio-Imaging Network; JH) and the Réseau de Recherche en Santé cardiométabolique, diabète et obésité (CMDO; JH).

Availability of data and material Statistical maps will be available upon reasonable request and released on Neurovault following publication. Raw data cannot be made available due to the ethical standards of the Ethics Committee of the University of Leipzig.

Declarations

Conflict of interest The author Arno Villringer has affiliations with the Max Planck Institute for Human Cognitive and Brain Sciences, Leipzig, Germany, the Clinic for Cognitive Neurology, University of Leipzig, Germany, the Leipzig University Medical Centre IFB Adiposity Diseases, Leipzig, Germany, and the Leipzig University Medical Centre Collaborative Research Centre 1052-A5, Leipzig, Germany. The author Christopher J. Steele has affiliations with Concordia University, Department of Psychology, Montreal, Canada and the Max Planck Institute for Human Cognitive and Brain Sciences, Leipzig, Germany. The author Christine L. Tardif has affiliations with McGill University, Department of Biomedical Engineering, Montreal, Canada and the Montreal Neurological Institute, Montreal, Canada. The author Pierre-Louis Bazin has affiliations with the University of Amsterdam, Faculty of Social and Behavioural Sciences, Amsterdam, Netherlands and the Max Planck Institute for Human Cognitive and Brain Sciences, Leipzig, Germany. The author Claudine J. Gauthier has affiliations with Concordia University, Department of Physics, Montreal, Canada and the Montreal Heart Institute, Montreal, Canada.

Ethical approval All procedures performed in studies involving human participants were in accordance with the ethical standards of the Ethics Committee of the University of Leipzig and with the 1964 Helsinki declaration and its later amendments. The study was approved by the Ethics Committee of the University of Leipzig.

References

Abdul-Kareem IA, Stancak A, Parkes LM, Al-Ameen M, AlGhamdi J, Aldhafeeri FM, Embleton K, Morris D, Sluming V (2011) Plasticity of the superior and middle cerebellar peduncles in musicians revealed by quantitative analysis of volume and number of streamlines based on diffusion tensor tractography. Cerebellum 10(3):611–623. https://doi.org/10.1007/s12311-011-0274-1

Albert NB, Robertson EM, Miall RC (2009) The resting human brain and motor learning. Curr Biol 19(12):1023–1027. https://doi.org/10.1016/j.cub.2009.04.028

Andersson JL, Sotiropoulos SN (2016) An integrated approach to correction for off-resonance effects and subject movement in diffusion MR imaging. Neuroimage 125:1063–1078

Andersson JL, Skare S, Ashburner J (2003) How to correct susceptibility distortions in spin-echo echo-planar images: application to diffusion tensor imaging. Neuroimage 20(2):870–888

Arsigny V, Fillard P, Pennec X, Ayache N (2006) Log-Euclidean metrics for fast and simple calculus on diffusion tensors. Magn Reson Med 56(2):411–421. https://doi.org/10.1002/mrm.20965

Avants BB, Epstein CL, Grossman M, Gee JC (2008) Symmetric diffeomorphic image registration with cross-correlation: evaluating automated labeling of elderly and neurodegenerative brain. Med Image Anal 12(1):26–41. https://doi.org/10.1016/j.media.2007.06.004

Avants BB, Tustison N, Johnson H (2009) Advanced normalization tools (ANTS). Insight J 2(365):1–35

Bassett DS, Yang M, Wymbs NF, Grafton ST (2015) Learning-induced autonomy of sensorimotor systems. Nat Neurosci 18(5):744–751. https://doi.org/10.1038/nn.3993

Beaulieu C (2002) The basis of anisotropic water diffusion in the nervous system—a technical review. NMR Biomed 15(7–8):435–455

Bengtsson SL, Nagy Z, Skare S, Forsman L, Forssberg H, Ullén F (2005) Extensive piano practicing has regionally specific effects on white matter development. Nat Neurosci 8(9):1148–1150. https://doi.org/10.1038/nn1516

Bloechle J, Huber S, Bahnmueller J, Rennig J, Willmes K, Cavdaroglu S, Moeller K, Klein E (2016) Fact learning in complex arithmetic—the role of the angular gyrus revisited. Hum Brain Mapp 37(9):3061–3079. https://doi.org/10.1002/hbm.23226

Braun C, Schweizer R, Elbert T, Birbaumer N, Taub E (2000) Differential activation in somatosensory cortex for different discrimination tasks. J Neurosci 20(1):446–450. https://doi.org/10.1523/JNEUROSCI.20-01-00446.2000

Briggs RG, Conner AK, Rahimi M, Sali G, Baker CM, Burks JD, Glenn CA, Battiste JD, Sughrue ME (2018) A connectomic atlas of the human cerebrum—chapter 14 tractographic description of the frontal aslant tract. Oper Neurosurg 15(suppl 1):444–449. https://doi.org/10.1093/ons/opy268

Briggs RG, Chakraborty AR, Anderson CD, Abraham CJ, Palejwala AH, Conner AK, Pelargos PE, O'Donoghue DL, Glenn CA, Sughrue ME (2019) Anatomy and white matter connections of the inferior frontal gyrus. Clin Anat 32(4):546–556. https://doi.org/10.1002/ca.23349

Caeyenberghs K, Metzler-Baddeley C, Foley S, Jones DK (2016) Dynamics of the human structural connectome underlying working memory training. J Neurosci 36(14):4056–4066. https://doi.org/10.1523/JNEUROSCI.1973-15.2016

Camus M, Ragert P, Vandermeeren Y, Cohen LG (2009) Mechanisms controlling motor output to a transfer hand after learning a sequential pinch force skill with the opposite hand. Clin Neurophysiol 120(10):1859–1865. https://doi.org/10.1016/j.clinph.2009.08.013

Catani M, Dell'Acqua F, Vergani F, Malik F, Hodge H, Roy P, Valabregue R, de Schotten MT (2012) Short frontal lobe connections of the human brain. Cortex 48(2):273–291. https://doi.org/10.1016/j.cortex.2011.12.001

Catani M, Robertsson N, Beyh A, Huynh V, de Requejo FS, Howells H, Barrett RL, Aiello M, Cavaliere C, Dyrby TB (2017) Short parietal lobe connections of the human and monkey brain. Cortex 97:339–357

Chanes L, Chica AB, Quentin R, Valero-Cabré A (2012) Manipulation of pre-target activity on the right frontal eye field enhances conscious visual perception in humans. PLoS ONE 7(5):e36232. https://doi.org/10.1371/journal.pone.0036232

Chéreau R, Saraceno GE, Angibaud J, Cattaert D, Nägerl UV (2017) Superresolution imaging reveals activity-dependent plasticity of axon morphology linked to changes in action potential conduction velocity. Proc Natl Acad Sci 114(6):1401–1406. https://doi.org/10.1073/pnas.1607541114

Chorghay Z, Káradóttir RT, Ruthazer ES (2018) White matter plasticity keeps the brain in tune: axons conduct while glia wrap. Front Cell Neurosci 12:428

Clark KL, Noudoost B, Moore T (2012) Persistent spatial information in the frontal eye field during object-based short-term memory. J Neurosci 32(32):10907–10914. https://doi.org/10.1523/JNEUROSCI.1450-12.2012

Cona G, Semenza C (2017) Supplementary motor area as key structure for domain-general sequence processing: a unified account. Neurosci Biobehav Rev 72:28–42. https://doi.org/10.1016/j.neubiorev.2016.10.033

Corbetta M, Shulman GL (2002) Control of goal-directed and stimulus-driven attention in the brain. Nat Rev Neurosci 3(3):201–215. https://doi.org/10.1038/nrn755

Costa RM, Cohen D, Nicolelis MAL (2004) Differential corticostriatal plasticity during fast and slow motor skill learning in mice. Curr Biol 14(13):1124–1134. https://doi.org/10.1016/j.cub.2004.06.053

Day JJ, Sweatt JD (2011) Epigenetic mechanisms in cognition. Neuron 70(5):813–829. https://doi.org/10.1016/j.neuron.2011.05.019

Dayan E, Cohen LG (2011) Neuroplasticity subserving motor skill learning. Neuron 72(3):443–454. https://doi.org/10.1016/j.neuron.2011.10.008

Deoni SCL, Rutt BK, Arun T, Pierpaoli C, Jones DK (2008) Gleaning multicomponent T1 and T2 information from steady-state imaging data. Magn Reson Med 60(6):1372–1387. https://doi.org/10.1002/mrm.21704

Dick AS, Garic D, Graziano P, Tremblay P (2019) The frontal aslant tract (FAT) and its role in speech, language and executive function. Cortex 111:148–163. https://doi.org/10.1016/j.cortex.2018.10.015

Ding Z, Gore JC, Anderson AW (2005) Reduction of noise in diffusion tensor images using anisotropic smoothing. Magn Reson Med 53(2):485–490. https://doi.org/10.1002/mrm.20339

Donner T, Kettermann A, Diesch E, Ostendorf F, Villringer A, Brandt SA (2000) Involvement of the human frontal eye field and multiple parietal areas in covert visual selection during conjunction search. Eur J Neurosci 12(9):3407–3414. https://doi.org/10.1046/j.1460-9568.2000.00223.x

Doyon J, Benali H (2005) Reorganization and plasticity in the adult brain during learning of motor skills. Curr Opin Neurobiol 15(2):161–167

Doyon J, Ungerleider LG, Squire L, Schacter D (2002) Functional anatomy of motor skill learning. Neuropsychol Mem 3:225–238

Doyon J, Bellec P, Amsel R, Penhune V, Monchi O, Carrier J, Lehéricy S, Benali H (2009) Contributions of the basal ganglia and functionally related brain structures to motor learning. Behav Brain Res 199(1):61–75. https://doi.org/10.1016/j.bbr.2008.11.012

Drevets WC, Burton H, Videen TO, Snyder AZ, Simpson JR, Raichle ME (1995) Blood flow changes in human somatosensory cortex during anticipated stimulation. Nature 373(6511):249–252. https://doi.org/10.1038/373249a0

Dumoulin SO, Fracasso A, van der Zwaag W, Siero JCW, Petridou N (2018) Ultra-high field MRI: advancing systems neuroscience towards mesoscopic human brain function. Neuroimage 168:345–357. https://doi.org/10.1016/j.neuroimage.2017.01.028

Fields RD (2015) A new mechanism of nervous system plasticity: activity-dependent myelination. Nat Rev Neurosci 16(12):756–767. https://doi.org/10.1038/nrn4023

Finc K, Bonna K, He X, Lydon-Staley DM, Kühn S, Duch W, Bassett DS (2020) Dynamic reconfiguration of functional brain networks during working memory training. Nat Commun 11(1):2435. https://doi.org/10.1038/s41467-020-15631-z

Forbes TA, Gallo V (2017) All wrapped up: environmental effects on myelination. Trends Neurosci 40(9):572–587. https://doi.org/10.1016/j.tins.2017.06.009

Frangou S, Doucet G, Lee W-H (2020) Myelination abnormalities in schizophrenia using ultra-high field MR brain imaging. Biol Psychiatry 87(9):S100–S101. https://doi.org/10.1016/j.biopsych.2020.02.276

Gaymard B, Ploner CJ, Rivaud-Péchoux S, Pierrot-Deseilligny C (1999) The frontal eye field is involved in spatial short-term memory but not in reflexive saccade inhibition. Exp Brain Res 129(2):288–301. https://doi.org/10.1007/s002210050899

Giacosa C, Karpati FJ, Foster NEV, Penhune VB, Hyde KL (2016) Dance and music training have different effects on white matter diffusivity in sensorimotor pathways. Neuroimage 135:273–286. https://doi.org/10.1016/j.neuroimage.2016.04.048

Giacosa C, Karpati FJ, Foster NEV, Hyde KL, Penhune VB (2019) The descending motor tracts are different in dancers and musicians. Brain Struct Funct 224(9):3229–3246. https://doi.org/10.1007/s00429-019-01963-0

Grosbras M-H, Paus T (2002) Transcranial magnetic stimulation of the human frontal eye field: effects on visual perception and attention. J Cogn Neurosci 14(7):1109–1120. https://doi.org/10.1162/089892902320474553

Gryga M, Taubert M, Dukart J, Vollmann H, Conde V, Sehm B, Villringer A, Ragert P (2012) Bidirectional gray matter changes after complex motor skill learning. Front Syst Neurosci 6:37

Guye M, Bettus G, Bartolomei F, Cozzone PJ (2010) Graph theoretical analysis of structural and functional connectivity MRI in normal and pathological brain networks. Magn Reson Mater Phys, Biol Med 23(5–6):409–421. https://doi.org/10.1007/s10334-010-0205-z

Halsband U, Lange RK (2006) Motor learning in man: a review of functional and clinical studies. J Physiol Paris 99(4–6):414–424

Hänggi J, Koeneke S, Bezzola L, Jäncke L (2010) Structural neuroplasticity in the sensorimotor network of professional female ballet dancers. Hum Brain Mapp 31(8):1196–1206. https://doi.org/10.1002/hbm.20928

Hardwick RM, Rottschy C, Miall RC, Eickhoff SB (2013) A quantitative meta-analysis and review of motor learning in the human brain. Neuroimage 67:283–297. https://doi.org/10.1016/j.neuroimage.2012.11.020

Heidemann RM, Anwander A, Feiweier T, Knösche TR, Turner R (2012) k-space and q-space: combining ultra-high spatial and angular resolution in diffusion imaging using ZOOPPA at 7T. Neuroimage 60(2):967–978. https://doi.org/10.1016/j.neuroimage.2011.12.081

Helms G, Dathe H, Kallenberg K, Dechent P (2008) High-resolution maps of magnetization transfer with inherent correction for RF inhomogeneity and T1 relaxation obtained from 3D FLASH MRI. Magn Res Med 60(6):1396–1407

Hikosaka O, Rand MK, Miyachi S, Miyashita K (1995) Learning of sequential movements in the monkey: process of learning and retention of memory. J Neurophysiol 74(4):1652–1661

Hikosaka O, Sakai K, Miyauchi S, Takino R, Sasaki Y, Putz B (1996) Activation of human presupplementary motor area in learning of sequential procedures: a functional MRI study. J Neurophysiol 76(1):617–621. https://doi.org/10.1152/jn.1996.76.1.617

Hikosaka O, Nakamura K, Sakai K, Nakahara H (2002) Central mechanisms of motor skill learning. Curr Opin Neurobiol 12(2):217–222. https://doi.org/10.1016/S0959-4388(02)00307-0

Hofstetter S, Tavor I, Moryosef ST, Assaf Y (2013) Short-term learning induces white matter plasticity in the fornix. J Neurosci 33(31):12844–12850. https://doi.org/10.1523/JNEUROSCI.4520-12.2013

Hyde KL, Lerch J, Norton A, Forgeard M, Winner E, Evans AC, Schlaug G (2009) Musical training shapes structural brain development. J Neurosci 29(10):3019–3025. https://doi.org/10.1523/JNEUROSCI.5118-08.2009

Imfeld A, Oechslin MS, Meyer M, Loenneker T, Jancke L (2009) White matter plasticity in the corticospinal tract of musicians: a diffusion tensor imaging study. Neuroimage 46(3):600–607. https://doi.org/10.1016/j.neuroimage.2009.02.025

Jaeger A-TP, Huntenburg JM, Tremblay SA, Schneider U, Grahl S, Huck J, Tardif CL, Villringer A, Gauthier CJ, Bazin P-L, Steele CJ (2021) Motor sequences—separating the sequence from the motor. A longitudinal rsfMRI study. BioRxiv. https://doi.org/10.1101/2021.02.09.430495

Jenkins IH, Brooks DJ, Nixon PD, Frackowiak RS, Passingham RE (1994) Motor sequence learning: a study with positron emission tomography. J Neurosci 14(6):3775–3790. https://doi.org/10.1523/JNEUROSCI.14-06-03775.1994

Jones DK, Symms MR, Cercignani M, Howard RJ (2005) The effect of filter size on VBM analyses of DT-MRI data. Neuroimage 26(2):546–554. https://doi.org/10.1016/j.neuroimage.2005.02.013

Karni A, Sagi D (1993) The time course of learning a visual skill. Nature 365(6443):250–252. https://doi.org/10.1038/365250a0

Karni A, Meyer G, Jezzard P, Adams MM, Turner R, Ungerleider LG (1995) Functional MRI evidence for adult motor cortex plasticity during motor skill learning. Nature 377(6545):155–158. https://doi.org/10.1038/377155a0

Kastrup A, Baudewig J, Schnaudigel S, Huonker R, Becker L, Sohns JM, Dechent P, Klingner C, Witte OW (2008) Behavioral correlates of negative BOLD signal changes in the primary somatosensory cortex. Neuroimage 41(4):1364–1371. https://doi.org/10.1016/j.neuroimage.2008.03.049

Klein E, Willmes K, Bieck SM, Bloechle J, Moeller K (2019) White matter neuro-plasticity in mental arithmetic: changes in hippocampal connectivity following arithmetic drill training. Cortex 114:115–123. https://doi.org/10.1016/j.cortex.2018.05.017

Knight RT, Staines WR, Swick D, Chao LL (1999) Prefrontal cortex regulates inhibition and excitation in distributed neural networks. Acta Physiol (Oxf) 101(2–3):159–178

Kohn KP, Underwood SM, Cooper MM (2018) Connecting structure-property and structure-function relationships across the disciplines of chemistry and biology: exploring student perceptions. CBE Life Sci Educ. https://doi.org/10.1187/cbe.18-01-0004

Korman M, Raz N, Flash T, Karni A (2003) Multiple shifts in the representation of a motor sequence during the acquisition of skilled performance. Proc Natl Acad Sci 100(21):12492–12497. https://doi.org/10.1073/pnas.2035019100

Krakauer JW, Hadjiosif AM, Xu J, Wong AL, Haith AM (2019) Motor learning. Compr Physiol 9(2):613–663. https://doi.org/10.1002/cphy.c170043

Lakhani B, Borich MR, Jackson JN, Wadden KP, Peters S, Villamayor A, MacKay AL, Vavasour IM, Rauscher A, Boyd LA (2016) Motor skill acquisition promotes human brain myelin plasticity. Neural Plast. https://doi.org/10.1155/2016/7526135

Lazari A, Koudelka S, Sampaio-Baptista C (2018) Experience-related reductions of myelin and axon diameter in adulthood. J Neurophysiol 120(4):1772–1775. https://doi.org/10.1152/jn.00070.2018

Le Bihan D, Mangin JF, Poupon C, Clark CA, Pappata S, Molko N, Chabriat H (2001) Diffusion tensor imaging: concepts and applications. J Magn Reson Imaging 13(4):534–546. https://doi.org/10.1002/jmri.1076

Lee S, Leach MK, Redmond SA, Chong SYC, Mellon SH, Tuck SJ, Feng Z-Q, Corey JM, Chan JR (2012) A culture system to study oligodendrocyte myelination processes using engineered nanofibers. Nat Methods 9(9):917–922. https://doi.org/10.1038/nmeth.2105

Lei Y, Perez MA (2017) Cortical contributions to sensory gating in the ipsilateral somatosensory cortex during voluntary activity. J Physiol 595(18):6203–6217. https://doi.org/10.1113/JP274504

Lenth R, Singmann H, Love J, Buerkner P, Herve M (2018) Emmeans: estimated marginal means, aka least-squares means. R Package Version 1(1):3

Lewis CM, Baldassarre A, Committeri G, Romani GL, Corbetta M (2009) Learning sculpts the spontaneous activity of the resting human brain. Proc Natl Acad Sci 106(41):17558–17563. https://doi.org/10.1073/pnas.0902455106

Liakakis G, Nickel J, Seitz RJ (2011) Diversity of the inferior frontal gyrus—a meta-analysis of neuroimaging studies. Behav Brain Res 225(1):341–347. https://doi.org/10.1016/j.bbr.2011.06.022

Lotze M, Scheler G, Tan H-R, Braun C, Birbaumer N (2003) The musician's brain: functional imaging of amateurs and professionals during performance and imagery. Neuroimage 20(3):1817–1829

Luft AR, Buitrago MM (2005) Stages of motor skill learning. Mol Neurobiol 32(3):205–216. https://doi.org/10.1385/MN:32:3:205

Marques JP, Kober T, Krueger G, van der Zwaag W, Van de Moortele P-F, Gruetter R (2010) MP2RAGE, a self bias-field corrected sequence for improved segmentation and T1-mapping at high field. Neuroimage 49(2):1271–1281

Miller EK, Cohen JD (2001) An integrative theory of prefrontal cortex function. Annu Rev Neurosci 24(1):167–202. https://doi.org/10.1146/annurev.neuro.24.1.167

Mohr H, Wolfensteller U, Betzel RF, Mišić B, Sporns O, Richiardi J, Ruge H (2016) Integration and segregation of large-scale brain networks during short-term task automatization. Nat Commun 7(1):13217. https://doi.org/10.1038/ncomms13217

Monfils M-H, Plautz EJ, Kleim JA (2005) In search of the motor engram: motor map plasticity as a mechanism for encoding motor experience. Neuroscientist 11(5):471–483. https://doi.org/10.1177/1073858405278015

Moraschi M, Hagberg GE, Paola MD, Spalletta G, Maraviglia B, Giove F (2010) Smoothing that does not blur: effects of the anisotropic approach for evaluating diffusion tensor imaging data in the clinic. J Magn Reson Imaging 31(3):690–697. https://doi.org/10.1002/jmri.22040

Mukherjee P, Chung SW, Berman JI, Hess CP, Henry RG (2008) Diffusion tensor MR imaging and fiber tractography: technical considerations. Am J Neuroradiol 29(5):843–852. https://doi.org/10.3174/ajnr.A1052

Nirkko AC, Ozdoba C, Redmond SM, Bürki M, Schroth G, Hess CW, Wiesendanger M (2001) Different ipsilateral representations for distal and proximal movements in the sensorimotor cortex: activation and deactivation patterns. Neuroimage 13(5):825–835. https://doi.org/10.1006/nimg.2000.0739

Nissen MJ, Bullemer P (1987) Attentional requirements of learning: evidence from performance measures. Cogn Psychol 19(1):1–32. https://doi.org/10.1016/0010-0285(87)90002-8

Pascual-Leone A, Amedi A, Fregni F, Merabet LB (2005) The plastic human brain cortex. Annu Rev Neurosci 28(1):377–401. https://doi.org/10.1146/annurev.neuro.27.070203.144216

Penhune VB, Steele CJ (2012) Parallel contributions of cerebellar, striatal and M1 mechanisms to motor sequence learning. Behav Brain Res 226(2):579–591

Poldrack RA (2000) Imaging brain plasticity: conceptual and methodological issues—a theoretical review. Neuroimage 12(1):1–13

Posner MI (1980) Orienting of attention. Q J Exp Psychol 32(1):3–25. https://doi.org/10.1080/00335558008248231

Riffert TW, Schreiber J, Anwander A, Knösche TR (2014) Beyond fractional anisotropy: extraction of bundle-specific structural metrics from crossing fiber models. Neuroimage 100:176–191. https://doi.org/10.1016/j.neuroimage.2014.06.015

Rioult-Pedotti M-S, Friedman D, Donoghue JP (2000) Learning-induced LTP in neocortex. Science 290(5491):533–536. https://doi.org/10.1126/science.290.5491.533

Sampaio-Baptista C, Johansen-Berg H (2017) White matter plasticity in the adult brain. Neuron 96(6):1239–1251

Sampaio-Baptista C, Vallès A, Khrapitchev AA, Akkermans G, Winkler AM, Foxley S, Sibson NR, Roberts M, Miller K, Diamond ME, Martens GJM, De Weerd P, Johansen-Berg H (2020) White matter structure and myelin-related gene expression alterations with experience in adult rats. Prog Neurobiol 187:101770. https://doi.org/10.1016/j.pneurobio.2020.101770

Savion-Lemieux T, Penhune VB (2005) The effects of practice and delay on motor skill learning and retention. Exp Brain Res 161(4):423–431

Schall JD (2004) On the role of frontal eye field in guiding attention and saccades. Vision Res 44(12):1453–1467. https://doi.org/10.1016/j.visres.2003.10.025

Schall JD, Bichot NP (1998) Neural correlates of visual and motor decision processes. Curr Opin Neurobiol 8(2):211–217. https://doi.org/10.1016/S0959-4388(98)80142-6

Schmithorst VJ, Wilke M (2002) Differences in white matter architecture between musicians and non-musicians: a diffusion tensor imaging study. Neurosci Lett 321(1):57–60. https://doi.org/10.1016/S0304-3940(02)00054-X

Scholz J, Klein MC, Behrens TE, Johansen-Berg H (2009) Training induces changes in white-matter architecture. Nat Neurosci 12(11):1370–1371

Seidler RD, Purushotham A, Kim S-G, Ugurbil K, Willingham D, Ashe J (2005) Neural correlates of encoding and expression in implicit sequence learning. Exp Brain Res 165(1):114–124. https://doi.org/10.1007/s00221-005-2284-z

Shima K, Tanji J (2000) Neuronal activity in the supplementary and presupplementary motor areas for temporal organization of multiple movements. J Neurophysiol 84(4):2148–2160. https://doi.org/10.1152/jn.2000.84.4.2148

Singmann H, Bolker B, Westfall J, Aust F, Ben-Shachar MS (2018) afex: analysis of factorial experiments. https://CRAN.R-project.org/package=afex. R package version 0.15-2

Skare S, Bammer R (2010) Jacobian weighting of distortion corrected EPI data. Positions 500(1):1

Smith SM, Jenkinson M, Woolrich MW, Beckmann CF, Behrens TE, Johansen-Berg H, Bannister PR, De Luca M, Drobnjak I, Flitney DE (2004) Advances in functional and structural MR image analysis and implementation as FSL. Neuroimage 23:S208–S219

Staines WR, Graham SJ, Black SE, McIlroy WE (2002) Task-relevant modulation of contralateral and ipsilateral primary somatosensory cortex and the role of a prefrontal-cortical sensory gating system. Neuroimage 15(1):190–199. https://doi.org/10.1006/nimg.2001.0953

Steele CJ, Zatorre RJ (2018) Practice makes plasticity. Nat Neurosci 21(12):1645–1646. https://doi.org/10.1038/s41593-018-0280-4

Steele CJ, Scholz J, Douaud G, Johansen-berg H, Penhune VB (2012) Structural correlates of skilled performance on a motor sequence task. Front Hum Neurosci. https://doi.org/10.3389/fnhum.2012.00289

Takeuchi H, Sekiguchi A, Taki Y, Yokoyama S, Yomogida Y, Komuro N, Yamanouchi T, Suzuki S, Kawashima R (2010) Training of working memory impacts structural connectivity. J Neurosci 30(9):3297–3303. https://doi.org/10.1523/JNEUROSCI.4611-09.2010

Tanji J (1996) New concepts of the supplementary motor area. Curr Opin Neurobiol 6(6):782–787. https://doi.org/10.1016/S0959-4388(96)80028-6

Tardif CL, Gauthier CJ, Steele CJ, Bazin P-L, Schäfer A, Schaefer A, Turner R, Villringer A (2016) Advanced MRI techniques to improve our understanding of experience-induced neuroplasticity. Neuroimage 131:55–72

Taylor PA, Saad ZS (2013) FATCAT: (an efficient) functional and tractographic connectivity analysis toolbox. Brain Connect 3(5):523–535. https://doi.org/10.1089/brain.2013.0154

Tournier J-D, Smith R, Raffelt D, Tabbara R, Dhollander T, Pietsch M, Christiaens D, Jeurissen B, Yeh C-H, Connelly A (2019) MRtrix3: a fast, flexible and open software framework for medical image processing and visualisation. Neuroimage 202:116137

Tustison NJ, Avants BB, Cook PA, Zheng Y, Egan A, Yushkevich PA, Gee JC (2010) N4ITK: improved N3 bias correction. IEEE Trans Med Imaging 29(6):1310–1320. https://doi.org/10.1109/TMI.2010.2046908

Van Hecke W, Leemans A, De Backer S, Jeurissen B, Parizel PM, Sijbers J (2010) Comparing isotropic and anisotropic smoothing for voxel-based DTI analyses: a simulation study. Hum Brain Mapp 31(1):98–114

van Mier H, Tempel LW, Perlmutter JS, Raichle ME, Petersen SE (1998) Changes in brain activity during motor learning measured with PET: effects of hand of performance and practice. J Neurophysiol 80(4):2177–2199. https://doi.org/10.1152/jn.1998.80.4.2177

Varriano F, Pascual-Diaz S, Prats-Galino A (2020) Distinct components in the right extended frontal aslant tract mediate language and working memory performance: a tractography-informed VBM study. Front Neuroanat. https://doi.org/10.3389/fnana.2020.00021

Vernet M, Quentin R, Chanes L, Mitsumasu A, Valero-Cabré A (2014) Frontal eye field, where art thou? Anatomy, function, and non-invasive manipulation of frontal regions involved in eye movements and associated cognitive operations. Front Integr Neurosci. https://doi.org/10.3389/fnint.2014.00066

Vidoni ED, Acerra NE, Dao E, Meehan SK, Boyd LA (2010) Role of the primary somatosensory cortex in motor learning: an rTMS study. Neurobiol Learn Mem 93(4):532–539. https://doi.org/10.1016/j.nlm.2010.01.011

Voldsbekk I, Maximov II, Zak N, Roelfs D, Geier O, Due-Tønnessen P, Elvsåshagen T, Strømstad M, Bjørnerud A, Groote I (2020) Evidence for wakefulness-related changes to extracellular space in human brain white matter from diffusion-weighted MRI. Neuroimage 212:116682. https://doi.org/10.1016/j.neuroimage.2020.116682

Vollmann H, Conde V, Sewerin S, Taubert M, Sehm B, Witte OW, Villringer A, Ragert P (2013) Anodal transcranial direct current stimulation (tDCS) over supplementary motor area (SMA) but not pre-SMA promotes short-term visuomotor learning. Brain Stimul 6(2):101–107. https://doi.org/10.1016/j.brs.2012.03.018

Wakana S, Caprihan A, Panzenboeck MM, Fallon JH, Perry M, Gollub RL, Hua K, Zhang J, Jiang H, Dubey P, Blitz A, van Zijl P, Mori S (2007) Reproducibility of quantitative tractography methods applied to cerebral white matter. Neuroimage 36(3):630–644. https://doi.org/10.1016/j.neuroimage.2007.02.049

Waxman SG (1975) Integrative properties and design principles of axons. Int Rev Neurobiol 18:1–40

Wei P, Bao R, Lv Z, Jing B (2018) Weak but critical links between primary somatosensory centers and motor cortex during movement. Front Hum Neurosci. https://doi.org/10.3389/fnhum.2018.00001

Weiskopf N, Mohammadi S, Lutti A, Callaghan MF (2015) Advances in MRI-based computational neuroanatomy: from morphometry to in-vivo histology. Curr Opin Neurol 28(4):313–322. https://doi.org/10.1097/WCO.0000000000000222

Wink AM, de Munck JC, van der Werf YD, van den Heuvel OA, Barkhof F (2012) Fast eigenvector centrality mapping of voxel-wise connectivity in functional magnetic resonance imaging: implementation, validation, and interpretation. Brain Connect 2(5):265–274. https://doi.org/10.1089/brain.2012.0087

Xu T, Yu X, Perlik AJ, Tobin WF, Zweig JA, Tennant K, Jones T, Zuo Y (2009) Rapid formation and selective stabilization of synapses for enduring motor memories. Nature 462(7275):915–919

Yamaguchi S, Knight RT (1990) Gating of somatosensory input by human prefrontal cortex. Brain Res 521(1):281–288. https://doi.org/10.1016/0006-8993(90)91553-S

Yokoi A, Arbuckle SA, Diedrichsen J (2018) The role of human primary motor cortex in the production of skilled finger sequences. J Neurosci 38(6):1430–1442

Zatorre RJ, Fields RD, Johansen-Berg H (2012) Plasticity in gray and white: neuroimaging changes in brain structure during learning. Nat Neurosci 15(4):528–536

Zhang H, Avants BB, Yushkevich PA, Woo JH, Wang S, McCluskey LF, Elman LB, Melhem ER, Gee JC (2007) High-dimensional spatial normalization of diffusion tensor images improves the detection of white matter differences: an example study using amyotrophic lateral sclerosis. IEEE Trans Med Imaging 26(11):1585–1597. https://doi.org/10.1109/TMI.2007.906784

Zhang H, Schneider T, Wheeler-Kingshott CA, Alexander DC (2012) NODDI: practical in vivo neurite orientation dispersion and density imaging of the human brain. Neuroimage 61(4):1000–1016. https://doi.org/10.1016/j.neuroimage.2012.03.072